Multiplex-edited mice recapitulate woolly mammoth hair phenotypes

Rui Chen[1†], Melissa L. Coquelin[1†], Kanokwan Srirattana[1], Rafael Vilar Sampaio[1], Jacob Weston[1], Rakesh Ganji[1], Raphael A. Wilson[1], Jessie Beebe[1], Alba Ledesma[1], Jacob Sullivan[1], Yiren Qin[1], J. Chris Chao[1], James B. Papizan[1], Anthony Mastracci IV[1], Ketaki Bhide[2], Jeremy Abraham Mathews[2], Gregory Knox[1], Rorie Oglesby[1], Mitra Menon[2], Tom van der Valk[3, 4,] Austin Bow[1], Brandi L. Cantarel[2], Matt W. James[1], James Kehler[1,5], Love Dalén[3, 4, 6], Ben Lamm[1,2], George M. Church[1, 2, 7], Beth Shapiro[1,*], Michael E. Abrams[1,8,*]

[1]Colossal Biosciences, Dallas TX, USA
[2]Form Bio, Dallas TX, USA
[3]Department of Bioinformatics and Genetics, Swedish Museum of Natural History, Stockholm, Sweden
[4]Centre for Palaeogenetics, Svanter Arrhenius väg 20C, Stockholm, Sweden
[5]UT Southwestern Medical Center, Dallas TX, USA
[6]Department of Zoology, Stockholm University, Stockholm, Sweden
[7]Department of Genetics, Harvard Medical School, Boston, MA, USA
[8]Lead contact
* Corresponding authors: mabrams@colossal.com; beth@colossal.com
† These authors contributed equally to this work

SUMMARY

The woolly mammoth (*Mammuthus primigenius*) possessed a thick woolly coat and other cold-adaptive traits that enabled survival in harsh arctic environments. Current de-extinction efforts focus on genetically modifying the closely related Asian elephant to express woolly mammoth traits. In this study, we establish a multiplex-edited mouse model with modifications in genes associated with hair morphology and lipid metabolism, enabling insights into traits involved in developing woolly hair textures. Our optimized workflows achieved high editing efficiencies and produced genetically modified mice with simultaneous editing of up to seven different genes. Selected modifications include loss-of-function mutations in *Fgf5, Tgm3*, and *Fam83g*, among others. The resulting mice display exaggerated hair phenotypes including curly, textured coats, and golden-brown hair. This study advances methods of rapid establishment of complex genetic models. These approaches inform de-extinction efforts and research involving the genetic basis of mammalian hair development.

KEYWORDS

CRISPR/Cas9, multiplexed gene editing, trait engineering, zygote editing, high-efficiency chimera, transgenic mice, hair, woolly mouse, mammoth, de-extinction

INTRODUCTION

One of the most prominent de-extinction efforts focuses on the woolly mammoth, *Mammuthus primigenius*, which disappeared following the extinction of the last surviving population on Wrangel Island approximately 4,000 years ago[1,2]. The mammoth de-extinction project aims to resurrect key mammoth traits such as woolly coats and other adaptations to cold habitats by genetically modifying mammoth-specific gene variants in the cells of the closely related Asian elephant, *Elephas maximus*. Genetic variants underlying phenotypes of interest are selected through comparative genomic analysis between the mammoth and elephant genomes[3]. Late-stage phases of the project involve somatic cell nuclear transfer of genetically modified Asian elephant cells, and subsequent surrogacy[4]. While active de-extinction efforts are underway with Asian elephant cells *in vitro*, phenotypic validation at the organism level faces significant challenges. The 22-month gestation period of elephants as well as their extended maturation timeline make rapid trait assessment impractical. Furthermore, ethical considerations regarding the experimental manipulation of elephants, an endangered species with complex social structures and high cognitive capabilities, necessitate alternative animal systems for proof-of-principle studies.

Mice are a well-defined model species with a 20-day gestation period, offering an ideal platform for refining methodologies and pipelines relevant for de-extinction. Specifically, workflows spanning targeted trait engineering, multiplex genome editing, high-efficiency animal generation, and non-invasive phenotypic assays can be rapidly implemented in mouse model systems. To this end, the CRISPR/Cas9 system has revolutionized the development of genetically modified mouse models[5,6], and over the last decade, an increasingly versatile toolkit for precise genetic modifications has been developed[7–10]. Multiple established techniques enable generation of gene-edited mice, including injection of CRISPR/Cas9-modified murine embryonic stem cells (mESCs) into blastocysts to generate chimeric animals[11], or direct zygote editing through CRISPR/Cas9 delivery[5,12,13].

Recent advances in genetic technology have improved our ability to create complex genetic models in mice, but challenges remain in making this process faster and more efficient. Traditional methods that inject mESCs into blastocysts only produce partially edited first-generation animals, requiring extensive breeding programs to create fully modified mice. While directly editing zygotes speeds up production time, it often results in mosaic patterns where not all cells contain the desired modifications[14,15]. Scientists have recently reduced mosaicism by injecting edited stem cells into 8-cell stage embryos[16,17], but this still requires the time-consuming process of creating fully modified stem cell lines with normal chromosomes. Improving these genetic engineering workflows is important not only for de-extinction projects but also benefits the broader scientific and industrial communities.

Here, we used a mouse model to 1) validate our multiplex genetic engineering pipelines; 2) demonstrate organism-level proof-of-principle trait engineering; and 3) produce mammoth-like genetic edits. We selected hair development as the primary trait of interest in this study. This rationale is multifactorial: hair offers a visual and diverse phenotype readout[18], murine hair development is well-characterized[19], and one of the most defining traits of the woolly mammoth is its dense coat[20]. Previous studies of mice have revealed mutations in genes that regulate distinct properties of hair, such as length (*Fgf5*[21]), pattern (*Tgm3*[22], *Fam83g*[23], *Fzd6*[24], *Krt25*[25], *Krt10*[26], *Tgfa*[27]), and color (*Mc1r*[28]) (**Figure 1A**). Using a trait engineering approach, we generated multiplex-edited mice with combinations of these mutations to evaluate whether a woolly coat phenotype could be engineered. We also selected two editing targets, *Krt27* and *Fabp2*, that parallel mammoth-specific variants from comparative analyses between mammoth and elephant genomes. We used optimized direct zygote editing (Experiments A-C) and high-efficiency chimera approaches (Experiments D-F) (**Figure 1B, Table S1**), enabling rapid (4-6 week) generation of multiplex-edited mice with as many as eleven edits in seven different genes. These novel combinations of genetic modifications yielded mice with varied hair phenotypes including woolly coat textures.

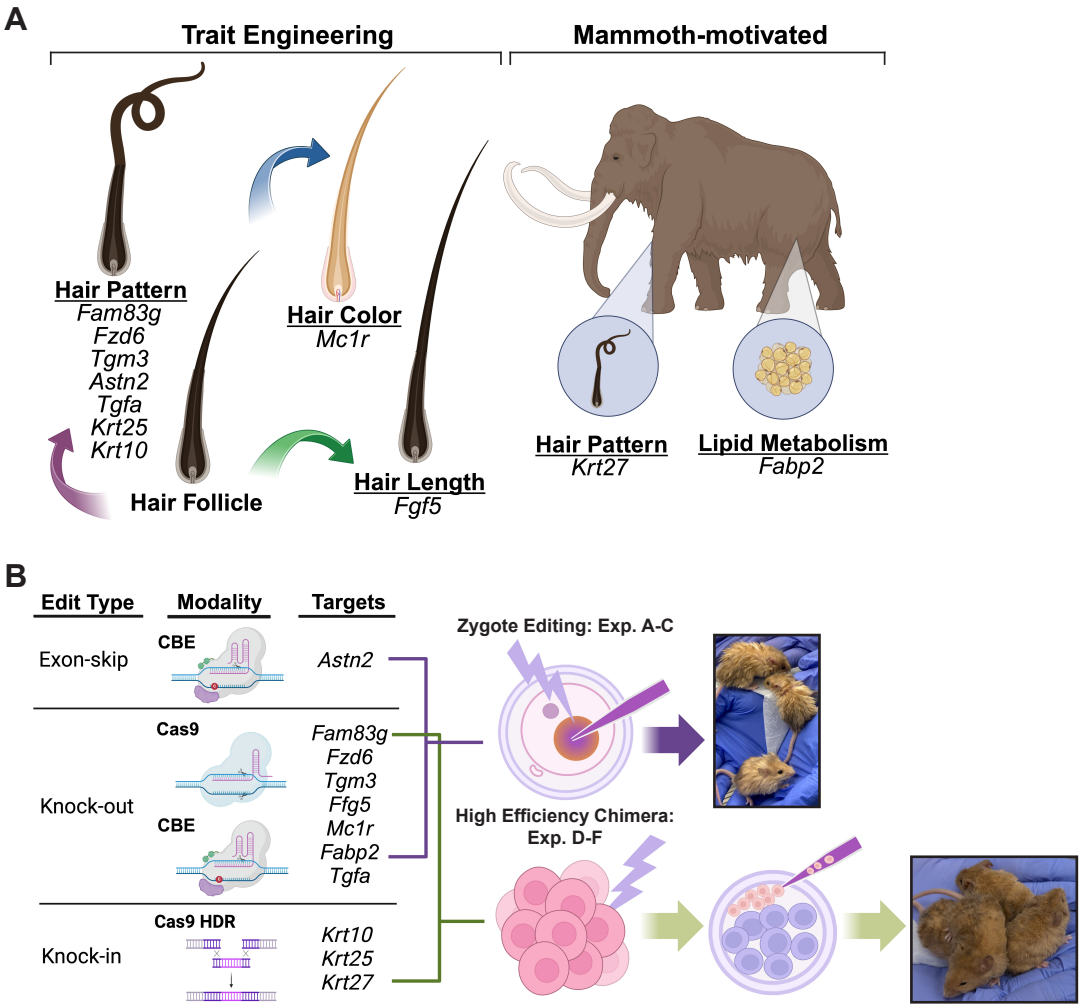

Figure 1. Overview of target traits, target genes, and editing workflows. Also see Table S1. **(A)** The target genes in this study fall into two categories: 1) woolly hair trait engineering based on existing literature, and 2) mammoth-motivated edits. **(B)** An illustration summarizing the editing modalities and two correlating animal generation workflows.

RESULTS

Rapid Generation of Woolly Mice via Multiplex Editing of Zygotes with CRISPR/Cas9

Electroporation of CRISPR/Cas9 ribonucleoprotein (RNP) complexes into mouse single-cell zygotes achieved efficient disruption of the six targeted genes: *Fgf5*, *Mc1r*, *Fam83g*, *Fzd6*, *Tgm3, and Fabp2* (**Figures 1B and 2A-B**). We carried out screening assays to prioritize sgRNAs based on three criteria: 1) high editing efficiency, 2) low predicted risk of off-target edits, and 3) targeting positions that either closely mimic previously reported mutations or that are in an early exon to facilitate full knock-out (KO).

To assess editing efficiency for multiple sgRNAs per target gene, we electroporated thawed B6C3F1 × B6D2F1 zygotes with Cas9 RNP complexes. We then cultured embryos to the blastocyst stage, followed by collection for genotyping (**Figure 2A**). **Figure 2B** shows the editing efficiencies (% total modifications and % KO) of each sgRNA, which ranged from undetectable to 100% editing and highlights sgRNAs selected for subsequent animal production in orange. Binding sites of the selected sgRNA within each target gene are shown in **Figure S1A**.

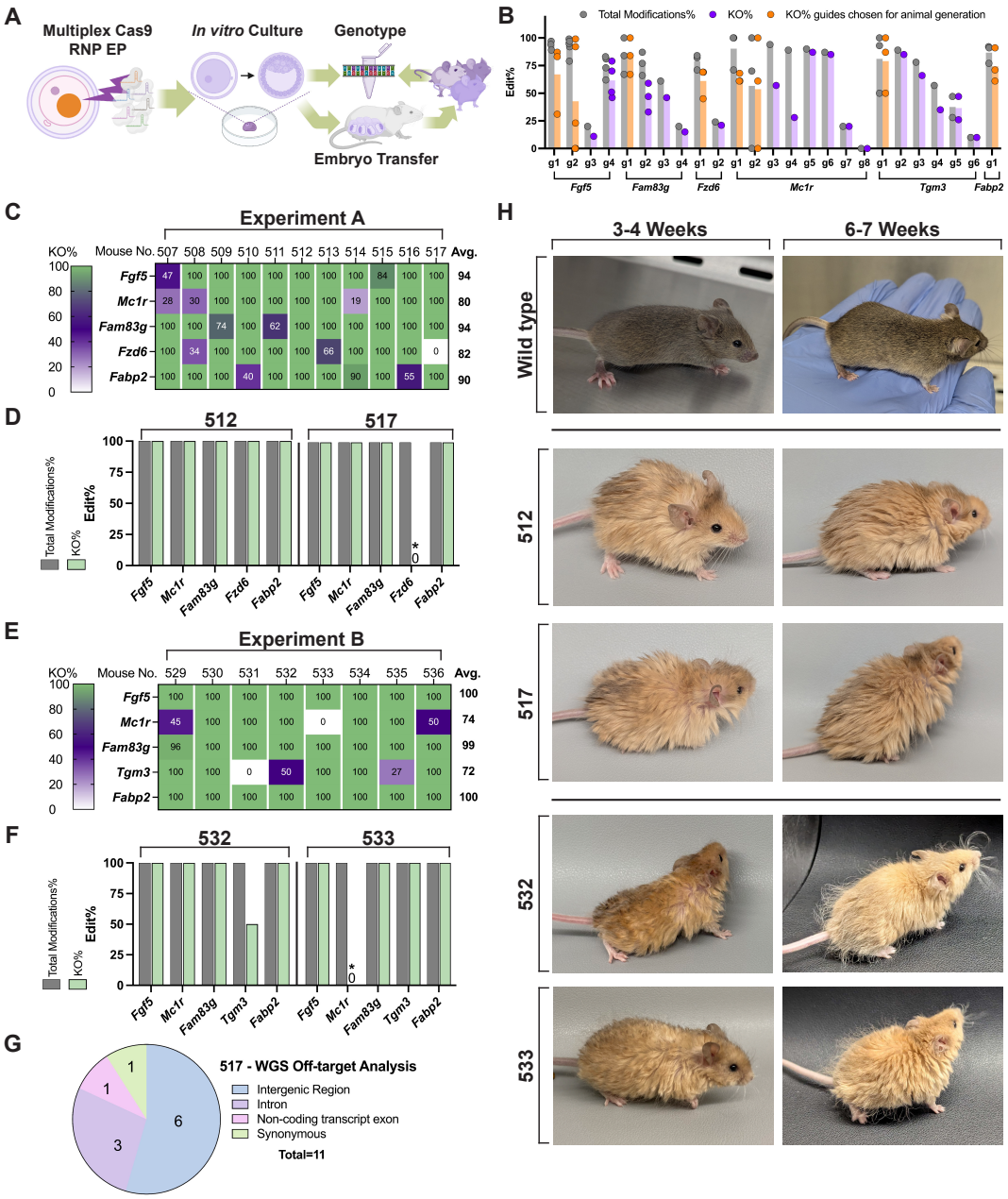

Figure 2. Experiments A and B: Gene editing in mice using CRISPR/Cas9 RNP zygote electroporation. (A) Workflow. We electroporated (EP) a pool of Cas9 RNPs with synthetic sgRNAs into wild-type mouse zygotes. We then cultured embryos into blastocyst stage *in vitro* and genotyped blastocysts to estimate editing efficiencies if needed. Next, we transferred blastocysts into surrogates for animal production experiments. Finally, we collected and genotyped ear punches from pups 21 days after birth. **(B)** Guide screening. We screened guides for editing efficiency in terminal experiments. For each guide, mean total modification efficiency (KO + unintended edits) is presented as a gray bar, KO efficiency as a purple bar for guides not selected for animal production experiments, and orange bar for guides selected for animal production experiments. Bars present average efficiencies from at least five embryos. Each circle represents an individual experiment that includes data from single embryos to pools of up to 18 embryos. **(C, E)** The KO% profiles of mice generated from Experiments A and B. Each column represents one mouse. "Mouse No." is the name of the mouse used in this study. **(D, F)** The total modifications% and KO% from mice #512 and #517 of Experiment A and #532 and #533 of Experiment B. "*" highlights the two in-frame homozygous edits in #517 (a 9 bp deletion in *Fzd6*) and #533 (a 21 bp deletion in *Mc1r*). **(G)** Editing off-target analysis by whole genome sequencing on mouse #517. **(H)** Photos of mice #512 and #517 of Experiment A and #532 and #533 of Experiment B at 3-4 weeks old and 6-7 weeks old. The wild-type reference photos are from age-matched agouti B6SJL F2.

We carried out two Cas9 editing animal production experiments using the selected sgRNAs. In Experiment A, we electroporated freshly collected B6SJLF2 zygotes with Cas9 RNPs and sgRNAs targeting *Fgf5*, *Mc1r*, *Fzd6, Fam83g*, *Fabp2*. Nearly half of the zygotes (63/134) developed to the blastocyst stage following electroporation (**Table S2**). We then transferred 60 blastocysts to three ICR pseudo-pregnant surrogates (**Figure 2A**). Eleven pups were born (18%; **Table S2**). Genotyping confirmed successful KO across all five target genes, with an average KO efficiency per gene across the 11 pups ranging from 80% for *Mc1r* to 94% for *Fam83g* (**Figure 2C**). Only modest mosaicism was detected: 54/55 of the possible target sites (5 targets x 11 mice) were 100% modified, and 42/55 had KO at 100%. The detailed genotypes of two representative mice, #512 and #517, are shown in **Figure 2D** and the remaining members of the litter are displayed in **Figure S1C**. All five target genes were fully disrupted in mouse #512, while mouse #517 had homozygous KOs for four target genes and a homozygous in-frame 9 bp deletion in *Fzd6*.

In Experiment B, we produced mice with simultaneous disruption (KO) of *Fgf5*, *Mc1r*, *Fam83g*, *Tgm3,* and *Fabp2* (**Figure 2E**). We electroporated zygotes as in Experiment A, resulting in a blastocyst formation rate of 56% (42/75; **Table S2**). Of these blastocysts, 28 were transferred to two ICR surrogates and eight pups were born, yielding a 29% birth rate (8/28; **Table S2**). Comparable levels of editing were achieved for the four gene targets in common with Experiment A. We detected little mosaicism, as 40/40 possible sites (8 mice x 5 targets) were fully modified, and only 6/40 had less than 95% KO. The unique target gene for this experiment, *Tgm3*, was edited at 100% in all eight mice, with 100% KO in five out of eight. The detailed genotypes of two mice, #532 and #533, are shown in **Figure 2F**, and the remaining members are shown in **Figure S1D**.

We performed short-read whole genome sequencing of mouse #517 to investigate the frequency of off-target edits. For the selected guides, computational analysis predicted 282 sites with three or fewer guide mismatches against the mouse genome where off-target edits were most likely to occur. We identified only 11 off-target edits in mouse #517 at these sites, none of which resulted in missense mutations (**Figure 2G**).

Experiments A and B produced mice with a variety of coat and eye colors determined by the status of *Mc1r* editing, and the genetic background of other coat/eye alleles in B6SJL F2 individuals (**Figures 2H** and **S1B-D**). Wild-type B6SJL F2 coat colors include agouti, black, white, light gray, and cream depending on which alleles for *Asip*, *Oca2*, and *Tyr* are inherited (**Figure S1B**)[29,30]. *Oca2*$^{p/p}$ mice have red eyes and light gray or cream coats, depending on which agouti (*Asip*) allele is present[31,32], while *Tyr*$^{c/c}$ mice have red eyes and white coats[33]. Unedited mice with agouti or black coats have black eyes[34]. *Mc1r* regulates pheomelanin and eumelanin and our intended disruption of *Mc1r* should only alter black or agouti coats to gold coats in black-eyed animals[28,35].

We successfully knocked out *Mc1r,* resulting in gold mice with black eyes. This phenotype is observed in mice #511, #512, #513, #516, #517, #532, #533, #534, and #535. Mice #509, #510, #515, and #530 were also homozygous knockouts at *Mc1r* but had white coats (**Figures S1C-D**), as expected in mice variants for albino coats[34]. Two mice with full editing of *Mc1r* did not show the expected coat color phenotype. Mouse #533 had a homozygous 21 bp in-frame deletion (**Figures 2F and 2H**), which was not considered a KO conventionally. However, mouse #533 still had a gold coat, indicating that the in-frame mutation nevertheless disrupted *Mc1r* function. Mouse #536 had a large deletion KO in one *Mc1r* allele, and also a 21 bp in-frame deletion in the other allele but had black hair (**Figure S1D**). The 21 bp *Mc1r* deletion in mouse #536 was, however, shifted by 9 bp compared to that of mouse #533. When we aligned both mutations to the wild-type MC1R protein (**Figure S1E**), we observed that the deletion in mouse #536 occurred near the second transmembrane domain of MC1R and spans the E92 residue, the loss of which has been associated previously with black coat color[36].

Both Experiments A and B generated founder mice with distinctive hair phenotypes, including increased length, altered texture, and enhanced waviness compared to wild type (**Figures 2H** and **S1C-D**). These phenotypes were consistent with previous reports describing disruptions to the individual target genes. For instance, *Fgf5* KO mice exhibited increased guard hair length, probably due to disruption of *Fgf5*-delayed anagen-catagen transition[21]. We observed a “feathered” hair texture in our *Fam83g*-edited mice, similar to

the *wooly* (*wly*) phenotype[23]. Mutations in *Tgm3* have previously been associated with changes to hair texture[22], and Experiment B mice with homozygous editing of *Tgm3* also exhibited wavy coats. Deletion of *Fzd6* has been shown to alter hair follicle orientation[24], and all mice with *Fzd6* knocked out displayed an exaggerated hair pattern phenotype. Given our shotgun-style multiplex strategy and the subsequently high gene editing efficiencies, it is difficult to assess the contribution of *Fzd6* disruption in the background of other gene knockouts. However, mice #517 (**Figures 2F and 2H**) and #513 (**Figure S1C**) had incomplete disruption of *Fzd6,* either as an in-frame mutation (#517) or mosaicism (#513) yet still presented with a woolly coat. These results suggest that *Fzd6* disruption did not significantly alter the macroscopic hair texture in our mouse model, and future experiments will be needed to fully characterize hair follicle orientation. Loss of *Fzd6* function did not compromise any exaggerated hair phenotype seen in Experiment A. Overall, the disruption of selected hair genes led to the successful generation of trait-engineered mice with woolly, gold coats.

Most mice from Experiment A and B had successfully engineered truncations of *Fabp2*, a mammoth-motivated gene candidate involved in fatty acid trafficking (**Figure 1A**). Mammoths have a fixed mutation in FABP2, resulting in an early stop codon and truncated protein[37]. In mice, KO of *Fabp2* leads to sex-dependent metabolic perturbations and differences in adiposity[38,39], suggesting a possible role in cold adaptation. All but two of the 19 mice in Experiments A and B were homozygously edited for the desired mutation of *Fabp2* (**Figures 2C and 2E**). In our small sample size, average mouse body mass did not significantly differ between gene-edited and wild-type mice fed a standard chow diet.

Rapid Generation of Woolly Mice via Multiplex Editing of Zygotes with a Fluorescence enriched Cytosine Base Editor Approach

In Experiment C, we used a cytosine base editor (CBE) to KO seven genes simultaneously: *Fgf5*, *Mc1r*, *Fam83g*, *Fzd6*, *Tgm3*, *Astn2*, and *Fabp2* (**Figures 1B and 3A**). CBE deaminates cytosine (C) to thymidine (T) within a defined targeting region[40]. CBE can therefore precisely install premature stop codons (*Fgf5*, *Mc1r*, *Fam83g*, *Fzd6*, *Tgm3*, and *Fabp2*)[41] or mutate splice sites for creating gene truncations (*Astn2*)[42,43] without eliciting double-stranded breaks[40].

To evaluate the efficiency of our CBE sgRNAs, we performed pronuclear injection (PNI) using thawed F2 hybrid zygotes with *in-vitro*-transcribed CBE mRNA and chemically synthesized sgRNA and collected embryos at the blastocyst stage for genotyping (**Figure 3A**). We found that cytosine deamination varied depending on the sgRNA and the target gene (**Figure 3B**). We prioritized sgRNAs for animal-production experiments (**Figure 3B** orange bars, **Figure S2A**) using the selection criteria described for Experiments A and B.

The co-expression of a red fluorescent protein, mScarlet3, via a P2A linkage was an effective reporter for CBE editing activity in zygotes (**Figures 3C-D and S2B-C**). We microinjected thawed F2 hybrid zygotes with CBE editor and multiplexed sgRNAs targeting *Fgf5*, *Fzd6*, *Fam83g*, *Tgm3*, and *Fabp2*. We manually sorted blastocysts into two groups based on the presence (+) or absence (-) of the red fluorescence signal. Genotyping analysis confirmed successful base editing in all red-fluorescent (+) embryos as well as high multiplexing in single embryos (**Figures 3D white dots, and S2B-C**). In contrast, embryos lacking red fluorescence (-) showed no detectable gene editing.

We leveraged the CBE reporter system to create mice edited at *Fgf5, Mc1r, Fam83g, Fzd6, Tgm3, Astn2*, and *Fabp2*. Fresh and thawed embryos exhibited comparable blastocyst formation rates: 70% (78/111) in fresh embryos and 71% (46/65) in thawed embryos (**Table S2**). Of these, the fluorescence rate of embryos was 65% (51/78) in fresh embryos and 35% (16/46) in thawed embryos. Five pups were obtained from the fresh zygote group after transferring 47 fluorescent embryos (11%; 5/47; **Table S2**), and three pups were born from the thawed group (33%; 3/9; **Table S2**). Every pup had at least heterozygous editing at more than one locus, and multiple pups were homozygous at 5 to 6 loci, with an average KO rate of 73% across six mice (**Figure 3E**). Average KO efficiencies per gene across all mice ranged from 59% for *Fzd6* to 91% for *Fgf5*. Mice #520 and #524 were edited at all seven genes. Mice #520 and #524 had homozygous KO for six genes and were heterozygous at a seventh, *Fzd6* and *Fam83g,* respectively (**Figure 3E**). Due to our

high editing efficiency and the nuclease-free nature of CBE, total gene editing (intended edits + bystander edits + indels) often matched precision stop codon installation, as few unintended insertions or deletions were detected (**Figure 3F**, #520).

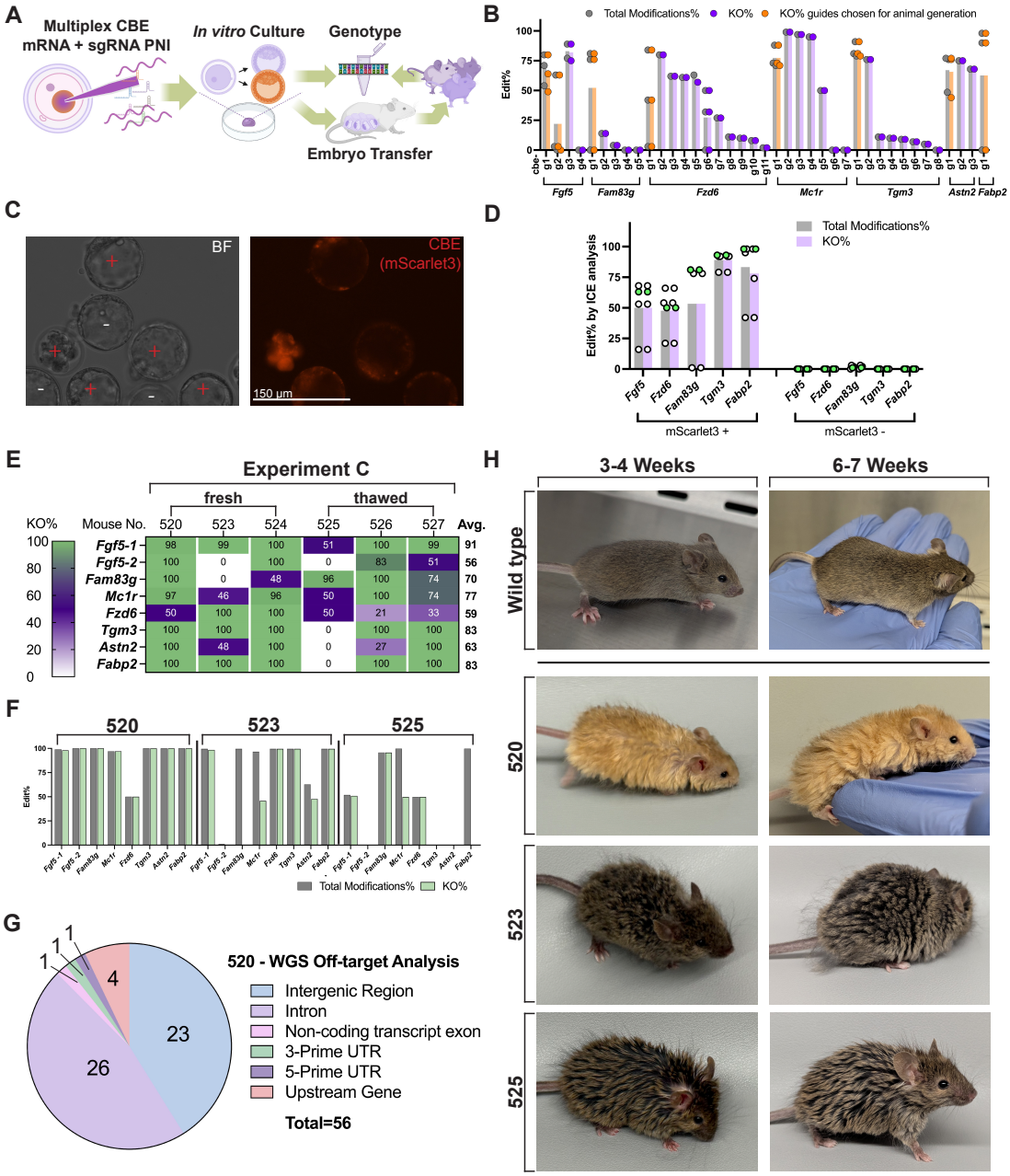

Figure 3. Experiment C: multiplex editing in mice using Cytosine Base Editor (CBE) PNI. (A) Workflow. We delivered a pool of CBE mRNA with sgRNAs into wild-type mouse zygotes by PNI. The mRNA transcript co-expresses CBE and a red fluorescent protein, mScarlet3. We cultured the embryos to the blastocyst stage *in vitro* and then evaluated mScarlet3 fluorescence. For screening experiments, we genotyped all blastocysts. For animal-producing experiments, we selected healthy blastocysts with bright mScarlet3 signals for transfer into surrogates. We collected ear punches for genotyping 21 days after the birth of the pups. **(B)** Guide screening. We screened guides for editing efficiency in terminal experiments. For each guide, mean total modification efficiency (KO + unintended edits) is presented as a gray bar, KO efficiency as a purple bar for guides not selected for animal production experiments, and an orange bar for guides selected for animal production experiments. Bars present average efficiencies measured from

at least six embryos. Each circle represents an individual experiment, including data from single embryos to pools of up to 19 embryos. **(C)** Fluorescent images of blastocysts after PNI of CBE-P2A-mScarlet3 mRNA and sgRNAs. Right: red signal from mScarlet3; left: bright field (BF) showing all embryos. "+" highlights the red embryos, and "-" highlights the non-red embryos. **(D)** Mean total modifications% (grey bars) and KO% (purple bars) comparison between mScarlet3+ and mScarlet3- embryos. Bars include data from at least seven embryos. White circles represent data from single embryos; green circles represent data from 6-8 pooled embryos. **(E)** The KO% profiles of mice generated from the CBE animal production Experiment C. Each column represents one mouse. "Mouse No." is the designated name of the mouse used in this study. **(F)** The total modification% and KO% from mouse #520, #523, and #525 from Experiment C. **(G)** Off-target analysis by whole genome sequencing on mouse #520. **(H)** Photos of mouse #520, #523, and #525, from Experiment C, taken at 3-4 weeks old and 6-7 weeks old. The wild-type reference photos are from age-matched agouti B6SJL F2; the same images as in Figure 2H.

Multiplexed CBE editing in zygotes led to few off-target edits. Our WGS analysis of 1,869 computationally predicted off-target sites revealed 56 total off-target edits in mouse #520 (**Figure 3G**), none of which resulted in missense mutations. The higher number of predicted and observed off-target sites in Experiment C compared to Cas9 editing in Experiment A was as expected due to the less-stringent PAM of the SpRY-based[44] editor that was employed, which provides flexibility in targeting but more promiscuous editing[45].

Experiment C produced mice with similarly altered phenotypes as in Experiments A and B (**Figures 3H and S2D**), and both fresh (#520, #523, #524) and thawed (#525, #526, #527) embryos generated mice with comparable genotype to phenotype correlations. We observed that the addition of early stop codons in *Fgf5, Fam83g, Fzd6,* and *Tgm3* and skipping an exon in *Astn2* yielded an exaggerated hair phenotype (**Figures 3F and 3H**). Due to the lower editing efficiency of *Mc1r* in Experiment C compared to Experiments A and B, we obtained more agouti mice. Interestingly, while mouse #525 had only a single gene homozygously knocked out – *Fam83g* – this mouse still had a feathered coat phenotype (**Figure 3F and 3H**). Mouse #523 was not edited at *Fam83g* (**Figure 3F**), and did not display a feathered coat, but rather had a frizzy/curly hair phenotype (**Figure 3H**), which may be due to the additive effects of *Fgf5, Fzd6,* or *Tgm3* disruption.

F0 Production of Woolly Mice with Near Full Contribution from Precision Edited mESCs

For Experiments D, E, and F, we established clonal mESCs modified with KO of *Fgf5*, *Mc1r*, *Fabp2, Tgfa*, *Fam83g, Fzd6,* and *Tgm3*, and knock-in (KI) of point mutations in the keratin family genes *Krt25*, *Krt27* and *Krt10* (**Figures 4A-B**), followed by high-yield chimera generation (**Figure 5A**). *Tgfa, Krt10, Krt25,* and *Krt27* were not genes modified in Experiments A-C. Tgfa is an EGFR ligand that plays a critical role in regulating hair development, and for which loss of function results in wavy hair textures[27,46]. We targeted an E172V substitution in *Krt10*, which has been associated with a "rough" coat texture, but normal hair length[26]. We separately targeted a L86Q substitution in *Krt25*, which has been linked to a wavy coat [25]. On the other hand, mammoth-motivated gene candidate *Krt27* was selected from our genomic analysis [37], which revealed that this gene had fixed protein coding variants in mammoths compared to Asian elephants. Specifically, mammoths have a valine at amino acid position 191 of KRT27, while Asian elephants have a methionine. Mutations in *Krt27* have previously been linked to hair phenotypes in mice[47]. To replicate the mammoth variant at this site, we introduced a valine at the same position in mouse *Krt27*, where wild-type mice have isoleucine (**Figure S3A**). We designed sgRNAs for Cas9 or CBE to target each gene (**Figures 4C-D**) as well as single-stranded oligonucleotide donors (ssODN) to act as HDR templates for *Krt10*, *Krt25,* and *Krt27* (**Figure 4C**). We used optimally performing guides and ssODNs (**Figures 4C-D orange bars, and S3C-D**) for subsequent mESC editing experiments. For use in these experiments, we derived a B6129 mESC line from freshly obtained mouse zygotes, enabling a low passage number starting point (see **Methods**).

We developed edited clonal mESC lines via three serial transfections targeting three different panels of gene combinations among Experiment D, E, and F (**Figure 4B**), consisting of four, four, and eleven edits, respectively. Each of these experiments included serial editing by RNP delivery. Additionally, the final transfection for Experiment F involved plasmid-based editing by CBE and a pair of 4-guide RNA arrays, coupled with enrichment by the BEAR (Base Editor Activity Reporter) reporting system[48] (**Figure S3B**). Post-transfection bulk cell populations exhibited edits at all desired loci with varying efficiencies (**Figure**

S3E). Bulk cell populations were sorted to isolate single-cell clones, followed by genotype screening (**Figures 4A and S3F**). To identify fully edited clonal lines, we evaluated the editing status of 45 mESC clones for Experiment D, 48 clones for Experiment E, and 43 clones for Experiment F. To expedite the initial genotype screen, we retained mESCs on irradiated mouse embryonic fibroblasts (iMEF) feeder layers and genotyped them by Sanger sequencing (**Figures S4A**). The carry-over of iMEF wild-type DNA and the detection limitation of ICE analysis for Sanger results may explain the distribution of editing (non-50% multiples) obtained. We re-genotyped promising candidates after culture on feeder-free laminin coated plates. We proceeded with highly modified clones that exhibited robust proliferation and excellent colony morphology - Clone 25 for Experiment D, Clone 14 for Experiment E, and Clone 20 for Experiment F (**Figures 4E and S4B**).

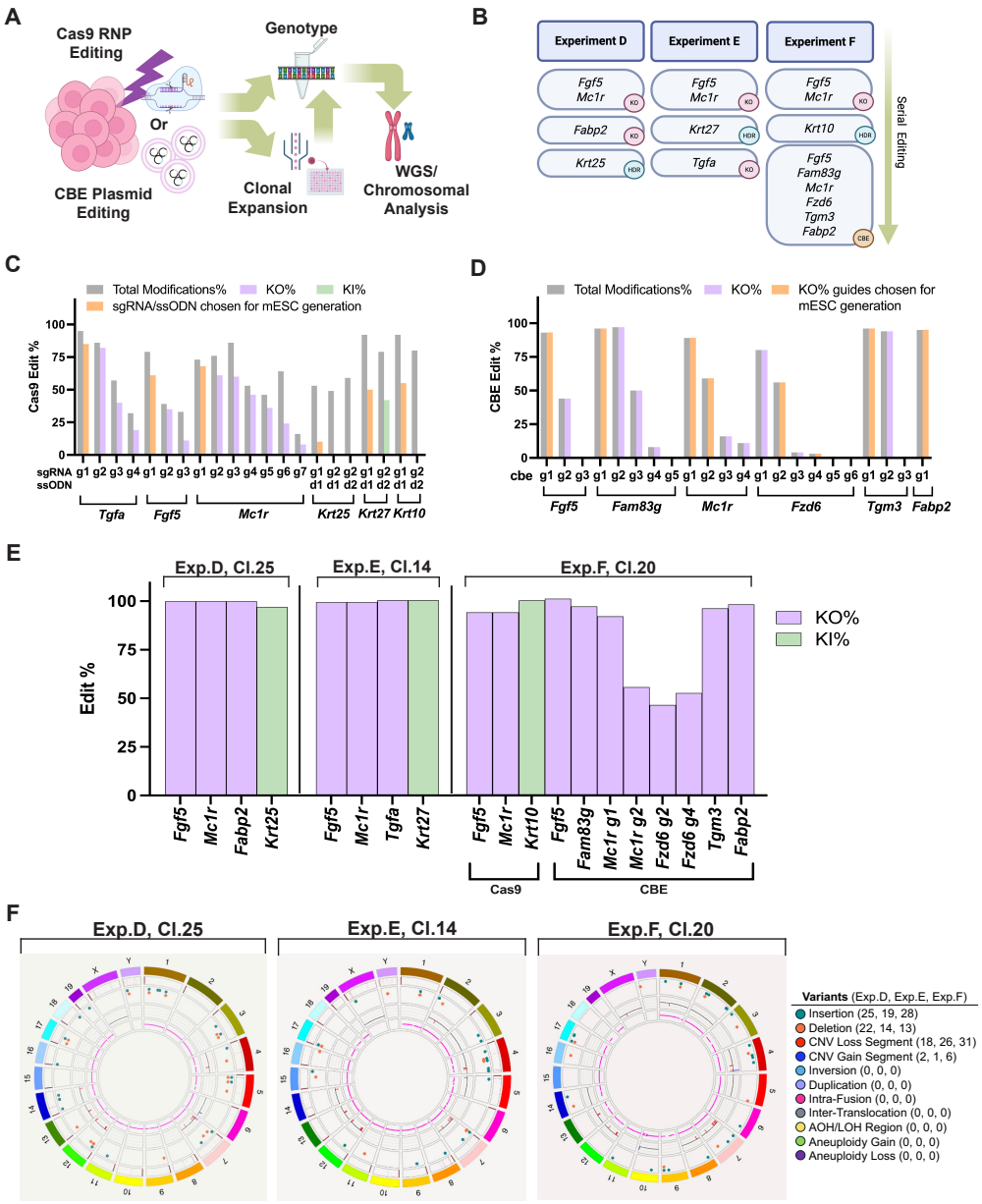

Figure 4. Experiment D, E, and F: generation of monoclonal, multiplex edited mouse embryonic stem cells using CRISPR/Cas9 RNP and CBE for woolly hair trait engineering. (A) Schematic for the generation of multiplex-edited monoclonal mESCs by CRISPR/Cas9 mediated KO or KI. We electroporated mESCs with Cas9 RNPs, sgRNAs

294 and ssODN (HDR template) or used Lipofectamine to deliver CBE and guide RNA plasmids. We collected cells 48
295 hours post-transfection for genotyping by Sanger sequencing. We also single-cell-sorted the bulk population of
296 transfected mESCs into 96-well plates containing iMEF feeders for clonal expansion, genotyping, and karyotyping. **(B)**
297 Flowchart depicting the sequential editing strategy used to generate multiplex-edited monoclonal mESC lines. **(C, D)**
298 Cas9 RNP guide, HDR ssODN, and CBE guide screening. Total modification efficiency is presented as a gray bar. KO
299 or KI efficiency is presented as a purple or green bar, respectively, for designs not selected for animal production
300 experiments, and an orange bar for designs selected for animal production experiments. Bars of each guide or each
301 guide-ssODN combination includes data from one experiment from two thousand mESCs. **(E)** Bar graph showing KO%
302 (purple) and KI% (green) for selected clonal lines generated in Experiments D, E, and F. We re-collected cells from
303 laminin-coated plates to ensure no iMEF contamination during secondary genotyping by Sanger sequencing. Editing
304 efficiencies were also confirmed by NGS. **(F)** Bionano Circos plot summarizing structural variations in Experiment D,
305 E, and F monoclonal mESC lines compared to the unedited WT cell line. Starting from the outer rings, the Circos tracks
306 depict 1. Cytoband, 2. mm39 DLE-1 SV mask, 3. Structural variants, 4. Copy number variants, and 5. Variant allele
307 fraction segments. Translocations would be depicted as curved lines across the center of the plot, though none were
308 detected in any sample. Numbers of variants are summarized on the right.

309 Whole genome sequencing data from the fully edited mESCs clonal lines and wild-type mESCs revealed
310 negligible off-target editing. As the edited clonal lines had the same genetic background (B6129), we were
311 able to carry out an unbiased genome-wide off-target analysis by comparison to the unedited mESC line.
312 We found limited high-impact off-targets, defined as splice modifying or protein coding variants. There were
313 none in Experiment D (Clone 25), one in Experiment E (Clone 14), and none in Experiment F (Clone 20)
314 (**Table S3**). Experiment E (Clone 14) had a single missense variant in the *Prkca* gene. The annotations for
315 all variants found in this analysis are summarized in **Table S3**.

316 The candidate clonal lines selected for animal generation maintained normal chromosome numbers, as
317 assessed by microscopy-based chromosome counting assays, PCR analysis, and Bionano optical genome
318 mapping. To evaluate the three clonal lines for common mESC aneuploidies[49], we performed Giemsa
319 staining and subsequent chromosomal counting (**Figure S4C**), and found no detectable loss of
320 chromosomes. PCR-based assessment of X and Y chromosomes showed retention of the Y chromosome
321 (**Figure S4D**), the loss of which is a common mESC aneuploidy[49]. We also performed comprehensive
322 structural genome analysis using Bionano (**Figure 4F**), which indicated that all 40 chromosomes were
323 present in each of the cell lines with no apparent aneuploidy, translocations, or other genomic abnormalities.
324 Copy number variants were minimal and often conserved between cell lines, including unedited B6129
325 mESCs, indicating that these variants were not caused by genetic editing.

326 The three edited mESC clones demonstrated robust high yield chimera formation, as each line produced
327 mice with near full mESC contribution via injection into 8-cell stage embryos (**Figure 5A**). We first
328 determined that mESCs localized to and formed the bulk of the inner cell mass by using a mESC line stably
329 expressing eGFP (**Figures 5B and S3B**). Next, we injected mESC clone 25 (Experiment D), clone 14
330 (Experiment E), and clone 20 (Experiment F) (**Figure 4E**) into wild-type 8-cell embryos. We observed that
331 98% (147/150) of the 8-cell stage embryos injected reached the blastocyst stage after two days in culture,
332 suggesting that *in vitro* embryo development was not negatively affected (**Table S2**). Between the three
333 experiments, we generated nine mice all edited at the expected level at each target site (**Figure 5C**). The
334 detailed genotypes of selected mice from Experiment D, E, and F are shown in **Figure 5D**, with the
335 remaining mice shown in **Figure S5**. Given that all mice born were male and their editing profiles exactly
336 matched that of the respective donor mESCs (**Figure 4E**), we infer that these mice were nearly 100% ESC-
337 derived.

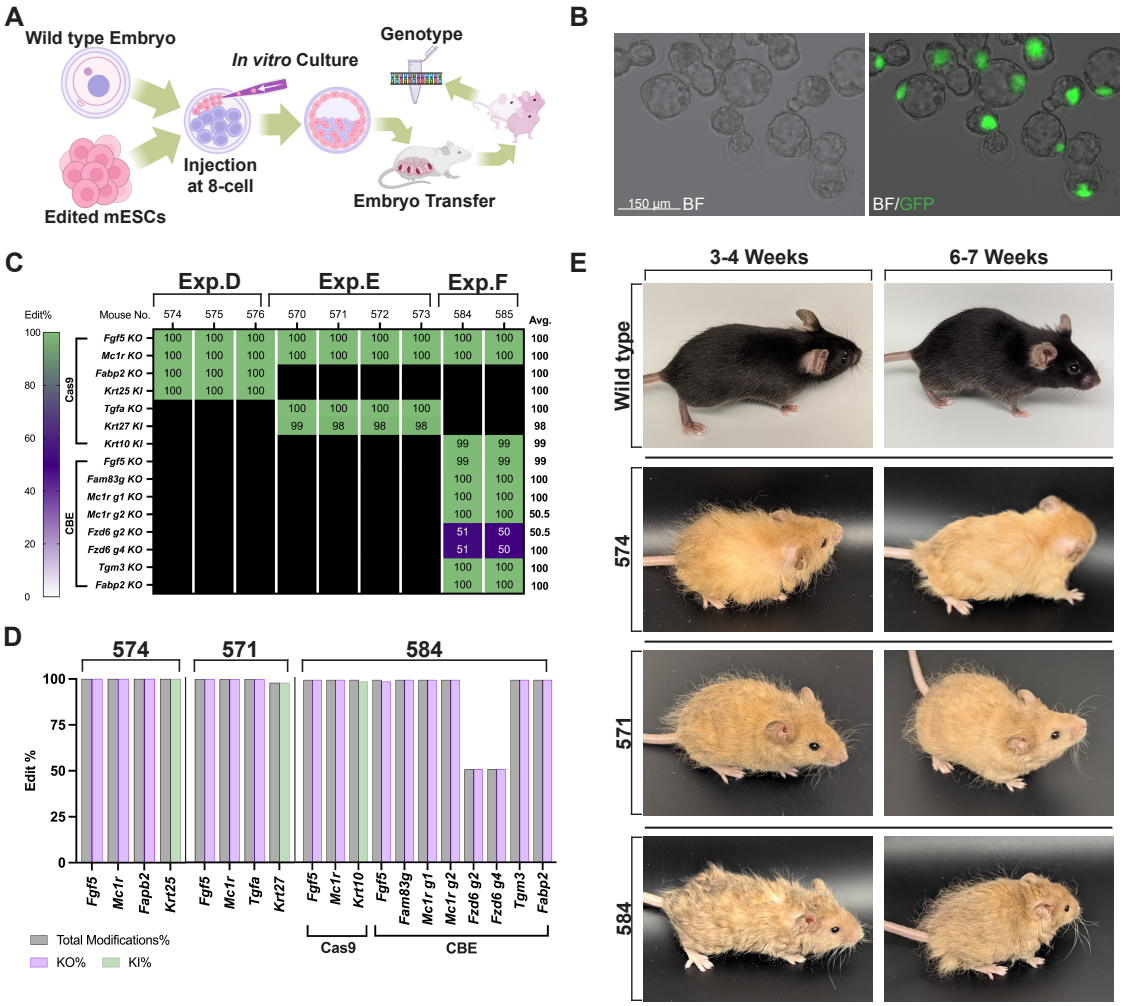

Figure 5. Experiment D, E, and F: generation of high yield woolly mouse chimeras using multiplex edited, monoclonal mouse embryonic stem cells. (A) Workflow for highly efficient production of edited mice within a single generation. We cultured edited monoclonal mouse ESCs in 2i medium and injected eight mESCs into an 8-cell stage zygote. We cultured the injected embryos in KSOM medium until the blastocyst stage and transferred the embryos to surrogates. Twenty-one days after birth, we collected ear punches for genotyping. **(B)** Representative image of blastocyst-stage embryos injected at the 8-cell stage with mESCs expressing GFP. Images taken at 20X. BF, bright field. **(C)** The KO% and KI% editing profile of mice generated from Experiment D, E, and F monoclonal cell lines. Each column is NGS data from n = 1 mouse. "Mouse No." is the name of the mouse used in this study. **(D)** The total modifications%, KO%, and KI% from mice #574 (Experiment D), #571 (Experiment E), and #584 (Experiment F). **(E)** Photos of mice #574 (Experiment D), #571 (Experiment E), and #584 (Experiment F) at 3-4 weeks old and 6-7 weeks old. Wild-type reference photos are from an age-matched C57BL/6N mouse.

Mice from Experiments D, E, and F had a gold coat, long guard hairs, and distinctive woolly hair textures (**Figures 5E and S5**). Mice from Experiment D (*Fgf5, Mc1r, Fabp2* KO; *Krt25* KI) (**Figure 5E,** #574) had a rough, wiry coat with disoriented hair. This wiriness diminished after six weeks of age and became more "Plush" in texture, as reported previously for this *Krt25* mutation [25]. Mice produced in Experiment E (*Fgf5, Mc1r, Tgfa* KO; *Krt27* KI) (**Figure 5E,** #571) had long, disordered guard hairs with a rough texture, as well as wavy hairs that remained closer in place to the body. Mice of Experiment F (*Fgf5*, *Mc1r*, *Fzd6*, *Fam83g*, *Tgm3*, *Fabp2* KO; *Krt10* KI) (**Figure 5E,** #584) had feathered, curly coats like mice from Experiment B or C, likely due to the shared targets. The phenotypes of mice produced within each experiment were strikingly similar to each other (**Figures 5E and S5A-C**), as expected due to the nearly full genetic contribution from

359 their respective clonal mESC lines. Overall, this workflow produced nine founder F0 mice with near-full
360 contribution from donor mESCs, with up to 11 edits across 7 genes and profound engineered woolly traits.

361 ***Successful Germline Transmission by Both Zygote-edited and mESC-derived F0 woolly mice***
362 We demonstrated successful germline transmission (**Figure 6**) produced by either zygote editing
363 (Experiment A-B; **Figure 2**) or mESC-based high efficiency chimera creation (Experiment D-F, **Figures 4-**
364 **5**). The F1 litters were healthy and had the expected genotype (**Figure 6A-D**) and phenotype (**Figure 6E**),
365 corresponding to each dam/sire cross.
366
367 To determine whether founder mice produced via zygote editing had germline gene modification, we set up
368 two crosses for mice from Experiment A and two crosses for mice from Experiment B. We mated mouse
369 #514 (dam) to either mouse #515 or #512 (sire). Dam #514 had ~20% mosaic *Mc1r* KO, as determined by
370 genotyping and observed by coat color pattern. All progeny from #514x#515 or #514x#512 were fully
371 modified at each gene (**Figure 6A**). However, mice #656 (#514x#512 progeny), #595, and #631 (#514x515
372 progeny) had heterozygous KO of *Mc1r* (**Figure 6B**). Consistent with this genotyping data, all progeny from
373 Experiment A founders had long woolly coat phenotypes, and all progeny but #595, #631, and #656 had
374 golden coat color (**Figure 6E**, #632 and #652, etc). Only progeny heterozygous for *Mc1r* had agouti color
375 (**Figure 6E**, #595, etc). Given these data, it is likely that dam #514 had higher *Mc1r* KO mosaicism in
376 gamete tissue compared to global editing. For Experiment B, we mated mouse #535 (sire) to either mouse
377 #534 or #536 (dam). Sire #535 had partial KO of *Tgm3*, dam #536 had partial *Mc1r* KO, as well as an allele
378 with a unique in-frame truncation (**Figures 6A-B and S1E**), and dam #534 had homozygous KO for all
379 targets. Progeny from the #534x#535 cross had 100% KO of each target gene (**Figure 6B**), and golden
380 woolly coats (**Figure 6E**, #640, etc). When dam #536 was crossed to sire #535, all progeny were 100%
381 modified across the five target genes, with expected alleles contributed from the dam and sire (**Figures**
382 **6A-B**). For example, the 21 bp in-frame deletion of *Mc1r* from the dam (#536) (**Figure S1E**) was inherited
383 by half the progeny (8/14, **Figure 6B**, #582-3, #588-9, #591-4). The coats of pups with these genotypes
384 were black (**Figure 6E**, #582, etc), further supporting the hypothesis that this *Mc1r* truncation spanning the
385 E92 residue generates black coats in a dominant manner over agouti coats. The other progeny (**Figure 6E**,
386 #580, etc.) showed the signature *Mcr1* KO-mediated gold coats, due to the frame-shifted *Mc1r* alleles from
387 founders #536 and #535. Demonstrated by F0 breeding, our high efficiency zygote editing pipeline rapidly
388 generated germ-line homozygous 5-plex gene knockout mouse models from a single generation.
389
390 Male F0 mice produced via mESC injection into 8-cell embryos (Experiment D, E and F) mated to wild-type
391 females produced F1 progeny (12/12 pups) that were heterozygous for the edits from the respective sires
392 (**Figure 6C**). Since *Mc1r* was heterozygous, the F1 progeny had either agouti (**Figure 6E**, #608, #603, etc)
393 or black coats (**Figure 6E**, #627, etc), depending on the coat color genetics of the wild-type dam.
394 Specifically, mice #574 and #570 were bred to agouti B6SJLF2 dams and #584 was bred to a black
395 B6SJLF2 dam. All progeny from the WTx#574 cross (Experiment D, 5/5) had a rough coat phenotype
396 (**Figure 6E**, #608, etc), while progeny from WTx#570 (Experiment E, 5/5) or WTx#584 (Experiment F, 2/2)
397 matings displayed no overt coat phenotype (**Figure 6E**, #603, #627, etc). All Experiment D F1 progeny had
398 the expected heterozygous KO or KI at all four targets (**Figure 6D**).

399 Some pups sired from mice of Experient E (sire #570) and F (sire #584) did not have the exact HDR-
400 mediated knock-in allele expected from the respective sire (**Figure 6D**). To investigate, we re-examined
401 the *Krt10* and *Krt27* loci in the DNA samples from these sires and their progeny and found a large 400-
402 500bp deletion. This deletion was not detected by our NGS genotyping strategy, as we employed a 300 bp
403 amplicon spanning the target site of interest (**Figure S6**). Our expanded genotyping data showed that sires
404 #570 and #584 were hemizygous for the precision edit in *Krt27* (#570) or *Krt10* (#584), with a deletion in
405 the alternate allele abolishing the primer binding site and therefore preventing amplification. Thus, progeny
406 inherited either the large deletion (**Figure 6D**, #603, #604, #607, #627, #628) or the precision edit (**Figure**
407 **6D**, #605, #606). Nevertheless, our mESC-based high-efficiency chimera pipeline achieved complete
408 germline penetration, correlating to the editing status of the sire.

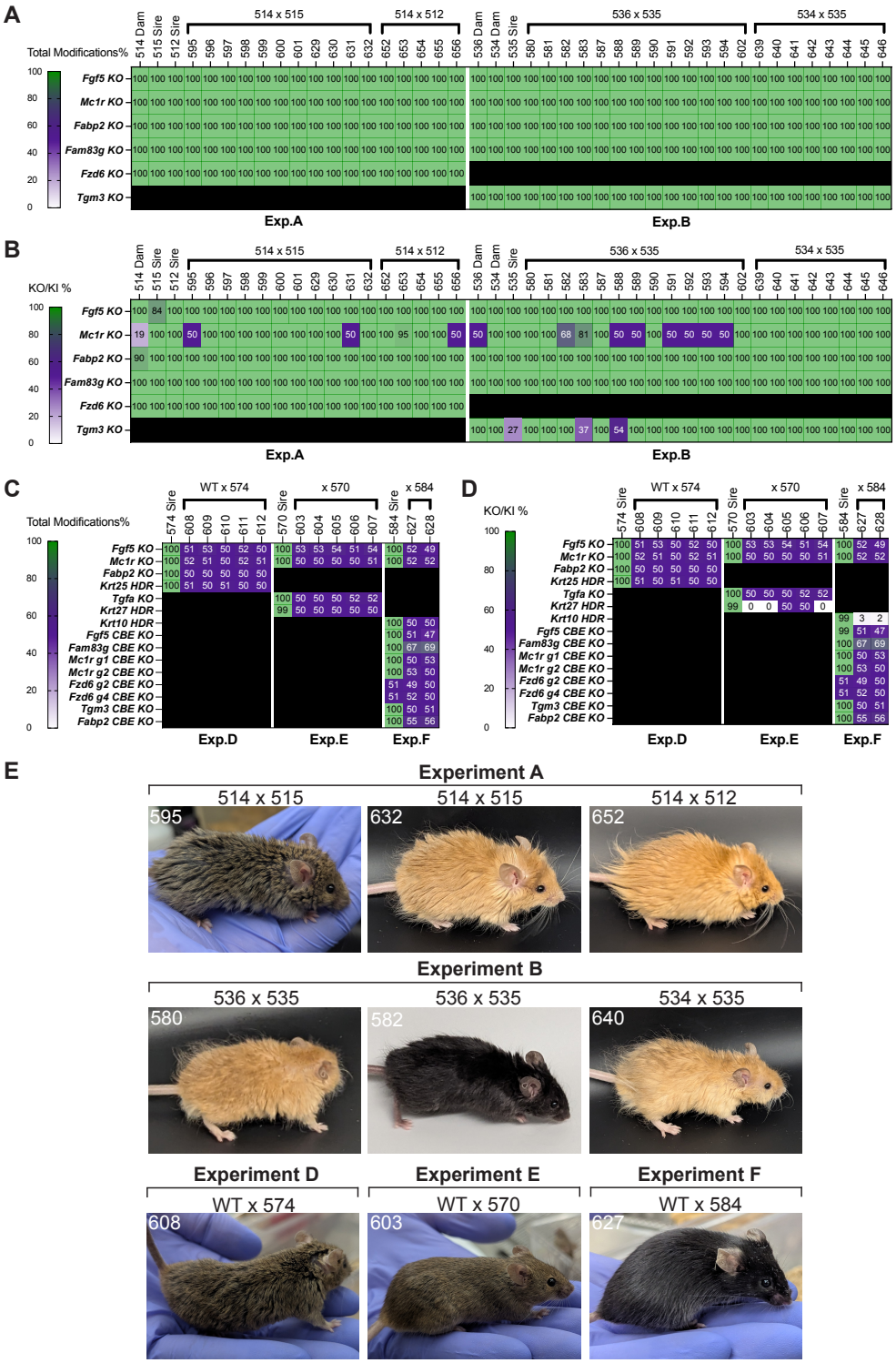

Figure 6. Germline editing is achieved by both zygote-edited and mESC-derived F0 woolly mice. (A, C) Total modification% or **(B, D)** desired edit (KI/KO) % of the dam, sire and their progeny from experiment A, B, D, E and F. #603, #604, #607, #627 and #628 inherited a large deletion on their HDR target, showing no KI. **(E)** Representative photos of F1 progeny from the breeding schemes of Experiment A and B (7-9 weeks) and Experiment D, E, and F (12-16 weeks).

DISCUSSION

We used several genome editing approaches to generate mice with combinatorial knock-outs or knock-ins in eleven genes involved in hair development and lipid metabolism (**Figures 1A-B**). The target genes were selected based on hair-associated mutations previously observed in mice, and mammoth-specific alleles identified through comparative genomic analysis. Our genetically modified mice have hair phenotypes including wiry coats, wavy hair, altered hair color, and woolly coats (**Figures 2H, 3H, 5E, S1C, S1D, S2D, and S5A-C**). Our mouse models provide validated animal production pipelines and demonstrated proof-of-concept trait engineering relevant to woolly mammoth de-extinction.

Our optimized protocols and workflows enabled the rapid and efficient production of multiplexed mouse models (**Figure 1B**). We found extensive guide screening essential to maintaining cost-effectiveness and minimizing zygote collections when generating genetically modified animals. Direct zygote editing with CRISPR/Cas9 enabled simultaneous KO of up to five genes with editing efficiencies exceeding 90% (**Figures 2C and 2E**). Similarly, CBE facilitated precise editing of eight target sites from seven genes simultaneously, while the fluorescent protein expression served as an effective reporter of editing success (**Figures 3C-E**). Importantly, high efficiency zygote editing resulted in germline modification, rapidly enabling F0 crosses to generate homozygously edited F1 offspring (**Figure 6A-B**). Our last strategy involved a two-step process: first mESCs were edited *in vitro*, and fully modified clones were identified; these clones were then injected into 8-cell embryos yielding chimera pups (**Figures 4A and 5A**). This approach yielded mice derived almost entirely from mESCs (**Figure 5C**), dramatically reducing the time needed to produce fully engineered mice and allowing F0 characterization of phenotypes[12,13,17,50,51]. Using a combination of RNP Cas9 KO, HDR, and base editing to genetically modify mESCs, we produced animals with up to eleven edits across seven target genes. Further, our high efficiency chimera method produced F0 animals with fully modified germ cells, and all edits were successfully inherited by every F1 progeny (**Figure 6C-D**).

Our mouse models provide evidence supporting the role of several spontaneous or induced mutations in genes involved in hair development, including *Fam83g*, *Tgm3*, and *Krt25*. The previously described “wooly” (*wly*) mutation arose spontaneously in a Jackson Laboratory colony. This phenotype is thought to be caused by altered splicing that leads to a frameshift mutation in exon 4 of *Fam83g*, although the researchers did not confirm this hypothesis by targeted gene knock-out[23]. Our *Fam83g* sgRNA used in Experiment A produces a similarly truncated protein by targeting the first few nucleotides of exon 3. Our study provides the first genetic validation that truncation of *Fam83g* alters hair texture. In *Tgm3,* multiple recessive wellhaarig (*we*) mutations are associated with wavy coats and curly vibrissae[22]. The we^{4j} variant has been fine-mapped to a 7 bp deletion in *Tgm3* that leads to a truncation after residue 512[22]. To our knowledge, the we^{4j} mutation has not been recapitulated by targeted CRISPR/Cas9 knockout. Our *Tgm3* sgRNA (Experiment B) targets within 40 bp downstream of we^{4j} , leading to a similar frameshift, supplying evidence that CRISPR/Cas9 mediated *Tgm3* truncation results in a wavy coat phenotype. The “Plush” mutation has previously been mapped to the *Krt25* gene in N-ethyl-N-nitrosourea (ENU)-induced mutant mice[25]. Mice from Experiment D had homozygous KI of L86Q in *Krt25*, precisely replicating the induced mutation. These mice also exhibited an initial wavy coat, followed by a more plush-like coat with aging (**Figure 5E,** #574, and **S5A**), consistent with previous observations[25], and thus provides evidence implicating the phenotypic effect of this substitution in *Krt25*. Another variant in *Krt25*, “Rex”, has been reported to result in curly coat phenotype in both heterozygotes and homozygotes[52]. Our F1 progeny from Experiment D also possessed a ruffled coat texture (**Figure 6E**, #608), probably from the dominant effect of heterozygous *Krt25* mutation.

The multiplexed editing strategies and mouse models established here provide a foundation for evaluating complex combinations of genetic modifications leading to woolly hair phenotypes. Findings from these experiments will continue to inform prioritization of genetic modifications for elephant cell engineering and mammoth de-extinction. Of course, while mouse models provide an experimentally tractable system for evaluating the functional consequences of genetic modifications, hair follicle biology and physiological parameters of mice probably differ from those of proboscideans, as they differ from those of humans[19]. Additionally, the mammoth cold-adaptive phenotype would have involved complex physiological

modifications beyond hair morphology, including changes in adipose distribution, vascular architecture, and metabolic thermoregulation. Nevertheless, the technical advances in multiplexed editing demonstrated here have implications for both basic research and therapeutic applications requiring precise orchestration of multiple genetic modifications.

RESOURCE AVAILABILITY

Lead Contact

Further information and requests for resources and reagents should be directed to and will be fulfilled by the lead contacts, Michael E. Abrams (mabrams@colossal.com) and Beth Shapiro (beth@colossal.com).

Materials availability

All unique/stable reagents generated in this study are available from the lead contact with a completed materials transfer agreement.

Data and code availability

Any additional information required to reanalyze the data reported in this paper is available from the lead contact upon request.

ACKNOWLEDGMENTS

The authors would like to thank Dr. Robert Hammer, John Ritter and the Transgenic Core at UTSW for their insight and support providing custom mouse model services. We would also like to thank Katie SoRelle, Faith McCorkle, and Lauren Pandolfo of the Colossal animal care team, and the staff at the Animal Resource Center at UTSW for their excellent care. We thank Dr. Eriona Hysolli for assistance with this work. Finally, we would like to thank Dr. Daniel Rokhsar, Dr. Andrew Pask, and Dr. Jun Wu for reviewing this work and for helpful comments on this manuscript. This work was supported by Colossal Biosciences.

AUTHOR CONTRIBUTIONS

Conceived and designed the experiments, performed experiments, carried out data analysis: R.C., M.L.C., K.S., R.V.S., R.A.W., R.G., J.W., A.L., J.B., J.S., A.B., and M.E.A; Cell culture and molecular biology experiments: R.C., M.L.C., R.A.W., R.G., J.W., J.B., J.S., G.K., and R.O.; Embryology experiments: K.S., R.V.S., A.L., and Y.Q.; Animal work: R.A.W., K.S., J.K., and M.W.J.; Bionano data acquisition and analysis: A.M.IV; NGS data acquisition: J.C.C., J.B.P., and A.M.IV; Bioinformatics analysis: K.B., J.A.M., M.M., J.W., and B.L.C.; Writing: R.C., M.L.C., K.S., R.V.S., R.A.W., R.G., J.W., A.L., J.B., J.S., B.S., and M.E.A.; Project supervision: B.C., M.J., J.K., B.L., G.M.C., B.S., and M.E.A.; Project conceptualization: B.L., G.M.C., B.S., L.D., T.v.d.V., and M.E.A.; Funding acquisition: B.L.; All authors were involved in reviewing and revising the manuscript.

DECLARATION OF INTERESTS

The authors have filed a patent application based on the results of this work. All authors are current or former employees, or scientific advisors/consultants for Colossal Biosciences and/or Form Bio, and may hold stock and/or stock options in these companies. G.M.C. is a founder and shareholder of Colossal Biosciences and others - full disclosure for G.M.C. is available at http://arep.med.harvard.edu/gmc/tech.html.

SUPPLEMENTAL INFORMATION

Document S1. Figures S1–S6 and Table S1-6 (Included in the main PDF)

MATERIALS AND METHODS

Animal housing and strains

Animal work described in this manuscript was approved and conducted under the oversight of the UT Southwestern Institutional Animal Care and Use Committee (IACUC) Dallas, TX, USA. All mice were housed in standard cages within a specific pathogen-free facility, maintained under a 12-hour light/dark cycle.

We used embryos from B6SJLF1 (The Jackson Laboratory, ME, USA) mice for zygote editing (Experiment A-C) and C57BL/6N (Charles River Laboratories, MA, USA) or B6SJLF1 mice for chimera generation (Experiment D-F). ICR (Inotiv, IN, USA) mice served as pseudopregnant recipients. We obtained frozen B6C3F1 × B6D2F1 embryos from Embryotech (MA, USA).

Pronuclear embryo production

Female B6SJLF1 mice (8–12 weeks old) were superovulated by administering 7.5 IU of pregnant mare serum gonadotropin (PMSG; Prospec, Rehovot, Israel), followed 48 hours later by 7.5 IU of human chorionic gonadotropin (hCG; Sigma-Aldrich, MO, USA). These females were then mated with male B6SJLF1 mice and fertilized embryos were collected from the oviducts 20 hours after the hCG injection. We maintained the harvested embryos in KSOM medium (EmbryoMax® Advanced KSOM Embryo Medium, Sigma-Aldrich, MO, USA). We obtained fertilized oocytes from C57BL/6N mice following the superovulation and mating protocol described above, except with 6.0 IU of PMSG followed by 6.0 IU hCG.

We thawed frozen B6C3F1 × B6D2F1 zygotes (Embryotech, MA, USA) at room temperature for 2 minutes, followed by washing and incubation in KSOM medium for 10 minutes at room temperature. We then cultured the zygotes in KSOM medium under mineral oil (Sigma-Aldrich, MO, USA) at 37°C in an atmosphere of 5% CO_2, 5% O_2, and 90% N_2 for one hour before proceeding with further experiments.

540 **Zygote electroporation and pronuclear injection**

541 We prepared RNP complexes for electroporation by preparing a mixture consisting of 1 μM recombinant *S.*
542 *pyogenes* Cas9 nuclease (Alt-R® S.p. HiFi Cas9 Nuclease V3, IDT, IA, USA), 1 μM of each sgRNA
543 (Synthego, CA, USA or IDT, IA, USA), and 4 μM Alt-R® Cas9 Electroporation Enhancer (IDT, IA, USA) in
544 OPTI-MEM® medium (Gibco, NY, USA). We placed zygotes (30–50) into a 0.1 cm-gap electroporation
545 cuvette (Bio-Rad, CA, USA) containing 10 μL of RNP complexes and performed electroporation at room
546 temperature using an ECM 2001 Electroporation System (BTX, MA, USA) with the following parameters:
547 30 V direct current, 3 ms pulse duration, and 5 pulses.

548 For pronuclear injection, we prepared a solution containing 200 ng/μL CBE mRNA and 25 ng/μL of each
549 sgRNA (Synthego, CA, USA or IDT, IA, USA) using nuclease-free water (Synthego, CA, USA). We injected
550 this solution into the pronuclei of zygotes placed in droplets of KSOM medium under mineral oil. We
551 performed microinjections using a FemtoJet 4i microinjector (Eppendorf, Hamburg, Germany) and a Nikon
552 ECLIPSE Ti2 inverted microscope (Nikon, Tokyo, Japan) equipped with micromanipulators (Narishige,
553 Ibaraki, Japan).

554 After electroporation and pronuclear injection, we cultured embryos in KSOM medium under mineral oil at
555 37°C in an atmosphere of 5% CO_2, 5% O_2, and 90% N_2 for 4 days. We then transferred blastocyst-stage
556 embryos into the uteri of pseudopregnant ICR mice at 2.5 days post coitum.

557

558 **Fluorescent imaging**

559 We imaged fluorescent blastocysts injected with CBE-mScarlet3 mRNA or injected with mESC expressing
560 GFP using the Invitrogen EVOS M7000 Imaging system (Thermo Fisher Scientific, MA, USA) equipped
561 with a 20X objective lens and RFP and GFP LED cubes.

562

563 **Murine embryonic stem cell (mESC) derivation**

564 We derived B6129 mESCs from hybrid F1-fertilized embryos generated by crossing C57BL/6J females with
565 129/S4 males. We collected one-cell zygotes from plugged females following treatment with PMSG
566 (Prospec, Rehovot, Israel) and hCG (Sigma-Aldrich, MO, USA), which we then cultured in advanced KSOM
567 medium (Sigma-Aldrich, MO, USA) until reaching the blastocyst stage at four days post-fertilization. We
568 removed the zona pellucida from the blastocysts via brief exposure to Tyrode's acidic solution (Sigma-
569 Aldrich, MO, USA). Zona-free blastocysts were collected using a mouth pipette, washed three times in
570 KSOM medium, and individually plated in 48-well plates containing inactivated mouse embryonic fibroblasts
571 (iMEFs, Thermo Fisher Scientific, MA, USA) and ESC derivation medium. The ESC derivation medium
572 consisted of Knockout Dulbecco's Modified Eagle Medium (KO-DMEM, Gibco, MA, USA) supplemented
573 with 20% Knockout Serum Replacement (KOSR, Gibco, MA, USA), recombinant mouse leukemia inhibitory
574 factor (LIF, Sigma-Aldrich, MO, USA), L-glutamine (Sigma-Aldrich, MO, USA), penicillin/streptomycin
575 (Sigma-Aldrich, MO, USA), non-essential amino acids (Sigma-Aldrich, MO, USA), and β-mercaptoethanol
576 (Sigma-Aldrich, MO, USA). After 7–8 days of culture, blastocyst outgrowths were enzymatically dissociated
577 using 0.025% trypsin solution (Sigma-Aldrich, MO, USA) for 10 minutes. We neutralized the trypsinization
578 reaction with ESC culture medium and the cells were then seeded onto 24-well plates pre-coated with
579 iMEFs. We subsequently expanded several ESC colonies to 6-well plates on iMEFs for further use. We
580 characterized ESC clonal lines for genomic stability, and selected a karyotypical male line at passage 2 for
581 editing and animal production in this study.

582

583 **mESC Culture**

584 We maintained B6129 mESCs on DR4 iMEFs at 37°C with 5% CO_2 in culture medium consisting of KO-
585 DMEM (Gibco, MA, USA) supplemented with 15% KOSR (Gibco, MA, USA), 1% GlutaMAX (Gibco, MA,
586 USA), 1% MEM Non-Essential Amino Acids (Gibco, MA, USA), 100 μM 2-Mercaptoethanol (Gibco, MA,
587 USA), 1000 U/mL LIF (Sigma-Aldrich, MO, USA), and 1% penicillin/streptomycin (Gibco, MA, USA),
588 changing the growth medium daily. We used collagenase (Gibco, MA, USA) to gently lift ESCs from the
589 iMEF feeder layer, followed by a brief incubation in diluted Accumax (Thermo Fisher Scientific, MA, CA) to
590 generate a single cell suspension for passaging and electroporation.

591

592 **Transfection of mESC cell lines**

593 We formed RNP complexes by combining 3200 ng of *S. pyogenes* Cas9 nuclease (Alt-R® S.p. HiFi Cas9
594 Nuclease V3, IDT, IA, US), 400 pmol of sgRNA (Synthego, CA, USA or IDT, IA, USA), and 5 μL of Alt-R®
595 Cas9 Electroporation Enhancer (IDT, IA, USA). For RNPs targeting HDR, we mixed an additional 400 pmol
596 of single-stranded DNA oligos (IDT, IA, USA) and 5 μL of Alt-R® Cas9 Electroporation Enhancer (IDT, IA,
597 USA) with Cas9 and sgRNA. Complexes were allowed to form for 10-20 minutes at room temperature.

598 For Cas9 editing, we electroporated RNP into 500K to 1M mESCs with the Lonza P3 Primary Cell 4D-
599 Nucleofector X Kit L (Lonza, Basel, Switzerland) using program CG104, according to the manufacturer's
600 protocol. Post electroporation, we seeded mESCs back on DR4 iMEFs in growth medium supplemented
601 with Y-27632 2HCL (Selleckem, TX, USA). For HDR experiments, we added 1 μM of Alt-R®HDR enhancer
602 (IDT, IA, USA) to the medium.

603 For CBE editing, we transfected plasmids into mESCs with Lipofectamine 2000 (Invitrogen, MA, USA)
604 according to the manufacturer's protocol. Briefly, we combined 4000 ng (1000 ng per plasmid) of CBE
605 editor, BEAR, and two multiguide cassette plasmids with Lipofectamine 2000 in OptiMEM reduced serum
606 medium (Gibco, MA, USA) at a wt/vol ratio of 1/3. Following DNA-lipofectamine complex formation, we
607 added the complex to 500K to 1M mESCs in suspension and incubated at 37°C with 5% CO_2 for 30 minutes.
608 Cells were then seeded back onto DR4 iMEFs following quick centrifugation to remove the DNA-
609 lipofectamine complexes.

610

611 **Clonal isolation of edited mESC lines**

612 After three serial rounds of electroporation as described above, we single-cell sorted mESCs directly onto
613 a 96-well plate pre-coated with iMEFs using the SONY SH800S sorter equipped with a 100 μM chip (SONY,
614 CA, USA). For the CBE editing experiment, only BEAR (GFP) and editor (mScarlet3) double positive cells
615 were selected for clonal outgrowth. We then expanded mESC colonies to a 24-well plate pre-coated with
616 DR4 iMEFs until approaching confluency. Ten percent of the mESCs were collected for Sanger sequencing.
617 The remaining ESCs were either cryopreserved in 90% KOSR/10% DMSO or seeded on laminin-coated
618 plates (Laminin-511, BioLamina, Sundyberg, Sweden) for downstream analysis. Selected mESC clones for
619 animal generation were thawed and expanded ten days before embryonic injection.

620

621 **Detection of Y chromosome by PCR**

622 We performed PCR on mESC clonal expansions to detect loss of the Y chromosome following established
623 primer designs[53]. We used a chromosomally normal male B6129 ESC line with an intact Y chromosome as

624 a positive control and a male B6129 ESC line with known Y chromosome loss as a negative control. We
625 performed a 15 µl PCR using KOD ONE (Sigma-Aldrich, MO, USA) as follows: 38-40 cycles of 98°C for 15
626 seconds, 60°C for 5 seconds, and 68°C for 5 seconds. We ran 10 µl of the resulting product on a 2%
627 agarose gel at 220 volts for 30 minutes, and obtained a gel image using the iBright. (Thermo Fisher
628 Scientific, MA, USA). Assuming no loss of the Y, the result should be a Y-chromosome specific amplicon
629 (280 bp) and two amplicons specific to the X chromosome (685 bp and 480 bp).

630

631 **Chromosome counting assay**

632 We performed chromosome counting of mESCs as previously described[54,55]. Briefly, we seeded clonal
633 mESC populations onto feeder-free laminin-coated (BioLamina, Sundyberg, Sweden) tissue culture plates
634 and maintained the cells in culture medium until cells reached confluency. We then added 200 ng/mL
635 colchicine (Sigma-Aldrich, MO, USA) to the culture medium and incubated cells at 37°C for 3 hours.
636 Following the incubation, we detached cells from the plate with 1:2 diluted Accumax (Thermo Fisher
637 Scientific, MA, USA) and prepared a single-cell suspension by pipetting. We then pelleted the cells via
638 centrifugation and subsequently resuspended the cells in 75 mM KCl. Following an incubation at 37°C for
639 8 minutes, we fixed cell suspensions in a 3:1 (v/v) solution of methanol and glacial acetic acid (Sigma-
640 Aldrich, MO, USA) at room temperature. Fixed cells were dropped onto glass slides and stained with
641 KaryoMAX Giemsa stain (ThermoFisher, MA, USA) in Gurr buffer (Gibco, MA, USA). We imaged stained
642 cells using bright-field microscopy (EVOS M7000) and counted chromosomes using the particle analysis
643 tool in the ImageJ software (v1.54f).

644

645 **Bionano analysis**

646 We performed bionano analysis of mESCs according to manufacturer specifications. Briefly, we pelleted
647 500K to 1M mESCs and isolated ultra high molecular weight (UHMW) genomic DNA as described in the
648 Bionano Prep SP-G2 Fresh Cell Pellet DNA Isolation Protocol (Bionano, Doc no. CG003). We then
649 fluorescently labeled UHMW gDNA by the Direct Label Enzyme (DLE-1) and then stained for backbone
650 visualization (Bionano Prep Direct Label and Stain (DLS) Protocol, Doc no. 30206). We loaded the labeled
651 and stained UHMW gDNA sample onto a Saphyr Chip and into the Saphyr System Instrument (Bionano
652 Saphyr System User Guide, Doc no. 30247). We used Bionano Solve to identify structural variations (SV)
653 and low variant allele fraction variants (VAF) (Bionano Solve Theory of Operation: Structural Variant Calling,
654 Doc no. CG-30110). We analyzed unedited mESCs in parallel as the background to extract SV information
655 for edited cell lines. The resolution for detecting variants with this method is ~500bp.

656

657 **Chimera production**

658 We maintained mESCs in the ground state of pluripotency for up to three passages in N2B27 basal medium,
659 modified from a previous publication[56], seven days before 8-cell stage injection. The medium comprised of
660 a 1:1 mixture of DMEM/F12 (Gibco, MA, USA) and Neurobasal (Gibco, MA, USA), supplemented with 1%
661 (v/v) B-27 (Gibco, MA, USA), 0.5% (v/v) N-2 (Gibco, MA, USA), 1% (v/v) GlutaMAX (Gibco, MA, USA), 2
662 mM MEM Non-Essential Amino Acids (Gibco, MA, USA), 100 U/mL Penicillin-Streptomycin (Sigma-Aldrich,
663 MO, USA), and 0.1 mM 2-mercaptoethanol (Sigma-Aldrich, MO, USA). Following Ying et al. 2008[57], we
664 further supplemented the medium with 1000 U/mL human LIF (Sigma-Aldrich, MO, USA) and the inhibitors
665 1 µM CHIR99021 (Selleckchem, TX, USA) and 0.4 µM PD0325901 (Selleckchem, TX, USA).

666 We produced chimeras by adapting the previously described laser-assisted protocol[16]. We cultured zygotes
667 from C57BL/6N mice in KSOM medium (Millipore, MA, USA) for approximately 48 hours at 37°C under 5%
668 CO_2 and 5% O_2. We selected embryos at the 8-cell stage, before compaction, for manipulation. Using a
669 holding pipette with 10-15 µm ID (Sunlight Medical, FL, USA) to stabilize the embryos, we made a
670 perforation in the zona pellucida (ZP) with an 800 ms tangential laser pulse (100% power) from an XYClone
671 laser system (Hamilton Thorne Bioscience, MA, USA), targeting the outer margin of the ZP in a region away
672 from blastomeres. We injected eight mESCs into the perivitelline space using an injection pipette with 15
673 µm ID (Sunlight Medical, FL, USA). Following injection, we washed the embryos and cultured them in
674 KSOM under the same environmental conditions. Embryos that developed into blastocysts were collected
675 and transferred to the uterine horns of pseudopregnant mice.

676

677 **Guide RNA and HDR donor design**

678 For Cas9 editing, we designed most synthetic single-guide RNA (sgRNA) using the CRISPR Predict tool in
679 Geneious Prime (Geneious, 2024.0.7) and others we manually designed. We assessed guide sites for
680 CRISPR activity using established efficiency scores[58]. We evaluated off-target effects against selected
681 regions of interest and the entire *Mus musculus* genome, GRCm39, with a tolerance of down to 3
682 mismatches. We further evaluated potential off-target edits in the Integrated DNA Technologies (IDT)
683 CRISPR-Cas9 guide RNA design checker (IDT, IA, USA). We designed ssODN templates for HDR
684 symmetrically around the cut site disrupted by the sgRNA. We used homology arms of thirty, forty, and sixty
685 base pairs and PAM silencing mutations for some donors.

686 For cytosine base editing (CBE), we designed sgRNAs to target regions where the C-to-T conversion would
687 either introduce a premature stop codon[41] or disrupt a splice site[43], both resulting in gene disruption and
688 loss of function. The editing designs in this study ensured that any C-to-T bystander effect from CBE would
689 not impede stop codon introduction or splice site mutation. However, edits other than C-to-T[59], although
690 less frequent, could abolish the effect of the intended point mutation. Unintended edits were considered
691 and evaluated during guide design and genotyping.

692 The sequences of all sgRNA and HDR donors used in this study are listed in **Tables S4 and S5**.

693

694 **Plasmids**

695 All plasmids were assembled via NEBuilder HiFi DNA Assembly (New England Biolabs (NEB), MA, USA).
696 Correct assembly was verified using Oxford Nanopore whole plasmid sequencing (Plasmidsaurus, OR,
697 USA). For zygote editing, we cloned an *in vitro* transcription plasmid template for CBE mRNA production.
698 This vector comprised a T7 promoter to initiate transcription, CBE-P2A-mScarlet3, and flanking UTR
699 sequences. For mESC editing, we cloned a CBE-P2A-mScarlet3 plasmid for base editor expression, four-
700 guide array plasmids for guide RNA driven by independent U6 promoters, a BEAR reporter plasmid for
701 base editing enrichment as previously described[48], and a eGFP integration piggyBAC plasmid for
702 generating a testing cell line of the high yield chimera workflow. We used Tad-CBEd[59] with a spRY PAM[44]
703 preference as the CBE of choice.

704

705

706

707 ***In vitro* transcription**

708 To produce the CBE mRNA used for zygote editing, we generated a linear DNA amplicon that included the
709 T7 promoter, coding regions, and UTRs using KOD One (Sigma-Aldrich, MO, USA) and a plasmid template.
710 We performed gel electrophoresis and excised the band corresponding to the amplicon, which we gel
711 purified using the QIAquick Gel Extraction Kit (Qiagen, MD, USA). We then bead purified the eluted DNA
712 using AMPure XP Beads (Beckman Coulter, CA, USA).

713 The purified amplicon served as a template for an *in vitro* transcription reaction using the HiScribe® T7
714 High Yield RNA Synthesis Kit (NEB, MA, USA). We incubated the reaction at 37°C for 2 hours, and then
715 purified mRNA using the Monarch RNA Cleanup Kit (NEB, MA, USA). We measured the yield and purity of
716 the mRNA using a Denovix DS-11 (Denovix Inc, DE, USA) and aliquoted purified mRNA, which we stored
717 at -80°C until use.

718

719 **Genotyping**

720 To collect samples for genotyping, we harvested embryos at the blastocyst stage, collected mESCs from
721 single-cell Accumax (Thermo Fisher Scientific, MA, CA) suspensions, and obtained ear notch samples from
722 individual mice 21–26 days after birth. We lysed each sample with Quick Extract (Fisher Scientific
723 Company, NH, USA) and placed each in a thermocycler at 65°C for 15 minutes followed by 98°C for 2
724 minutes.

725 We amplified genomic regions spanning the mutation of interest via PCR, followed by next generation
726 sequencing (NGS) or Sanger sequencing as described below. All primer sequences used for genotyping
727 are listed in **Table S6** and were designed in Geneious Prime (Geneious, 2024.0.7).

728 To prepare amplicons for NGS genotyping, we performed two step PCR. PCR1 used KOD ONE (Sigma-
729 Aldrich, MO, USA) and a thermocycle consisting of 30-35 cycles of 98°C for 15 seconds, 60°C for 5
730 seconds, and 68°C for 5 seconds. We added 1 µl of PCR1 into the PCR2 mixture that included custom
731 indexes for i5 and i7 adapter sequences (IDT, IA, USA). The PCR2 thermocycle consisted of 8 cycles of
732 98°C for 15 seconds, 60°C for 5 seconds, and 68°C for 5 seconds. We confirmed amplification via gel
733 electrophoresis with 5 µl of PCR2.

734 Next, we pooled PCR2 samples into a purified library pool using AMPure XP Beads (Beckman Coulter, CA,
735 USA) at 1:1 ratio, quantified DNA concentration by both Qubit Flex Fluorometer (Thermo Fisher Scientific,
736 MA, USA), and visualized library amplicon size with a D1000 ScreenTape (Agilent Technologies, CA, USA)
737 on the Agilent TapeStation. We sequenced libraries using either a 300- or 500-cycle kit on the Illumina
738 MiSeq or the NextSeq2000 instruments (Illumina, CA, USA) targeting ten thousand reads per sample. We
739 uploaded the data onto the Form Bio (Form Bio Inc., TX, USA) platform and ran the VALID workflow. Briefly,
740 sequence read pairs are merged using fastp[60], then reads are aligned to the expected amplicons using
741 Magic-blast[61] for edited and wild-type cells. We used these alignments to calculate editing efficiencies and
742 identify off-target edits overlapping the amplicon region.

743 For Sanger sequencing, we performed 15 µl PCRs using KOD ONE (Sigma-Aldrich, MO, USA) as follows:
744 38-40 cycles of 98°C for 15 seconds, 60°C for 5 seconds, and 68°C for 5 seconds. After PCR was complete,
745 we ran 5 µl of the samples on a 2% agarose gel to confirm presence of a band. We sent the remaining 10
746 µl of the unpurified PCR to Genewiz/Azenta (Genewiz/Azenta, NJ, USA) for Sanger sequencing. We ran
747 ab1 files from Sanger sequencing on the Synthego website for ICE Analysis.

748 We define gene knock-out (KO) as exonic insertions or deletions (indels) not in multiples of three, an exonic
749 indel over 100 bp, introduction of a stop codon, or a splice site mutation. For large indels that may influence

750 the mapping of NGS reads (usually >100 bp), we used electrophoresis band patterning and Sanger
751 sequencing to confirm absence of wild-type sequences. All mice were genotyped primarily by NGS and
752 supplemented by band patterning and Sanger sequencing.

753

754 **Whole genome sequencing and off-target analysis**

755 For each sample, we extracted genomic DNA using the NucleoSpin Tissue kit following manufacturer
756 instructions (Macherey-Nagel, Düren, Germany). Libraries were prepared using the Illumina DNA Prep kit
757 (Illumina, CA, USA). We used double-sided bead purification to purify amplified libraries which we quantified
758 using an Agilent TapeStation (Agilent Technologies, CA, USA) prior to normalization and pooling. Libraries
759 were then sequenced on the NextSeq2000 (Illumina, CA, USA) using XLEAP-SBS chemistry targeting 30x
760 genomic coverage per sample.

761 We identified editing at off-target sites by whole genome sequencing and alignment. We used the Valid
762 WGS workflow on the Form Bio platform to identify SNVs, indels, and structural variants to identify edits. In
763 this workflow, we trimmed reads using fastp and then aligned them to the mm39 reference genome[62] using
764 Sentieon optimized BWA MEM[63,64]. Duplicate reads were marked using Picard MarkDuplicates. Somatic
765 variants were detected using the Sentieon TNHaplotyper2 tool while structural variant calls were detected
766 using DNAscope. We filtered variants based on multiple filtering criteria (Strand bias, Alternate Allele Count
767 < 2, Variant Allele Frequency < 0.7) to predict on and off target edits. After filtering, on target and off target
768 variants list were split based on the intended location of on targets. Quality reports were produced by
769 MultiQC. Variant effects were determined using snpEff.

770 For zygote editing, we took a targeted approach to determine off-target editing to account for normal genetic
771 variations between individuals. We predicted off-target binding sites for all multiplexed guides in each
772 zygote-editing experiment using the Form Bio platform (Formbio, Texas, USA) via the DR GENE workflow,
773 which uses an in-house implementation of the runCrisprBwa function from the crisprVerse package in R[65].
774 All predicted off-target sites with three or fewer mismatches to the sgRNA protospacers were interrogated
775 for off-target editing from the WGS data. For mice produced from CBE-edited zygotes, variants found within
776 ±20bp of a predicted off-target binding site were considered off-target edits. To account for larger potential
777 alterations due to NHEJ in the mice produced from Cas9-edited zygotes, variants found within ±200bp of a
778 predicted off-target binding site were considered off-target edits. Of these, all variants with a VAF greater
779 than 0.7 and read depth greater than 5 are reported. As ESC and ESC derived samples originate from the
780 same B6129 ESC cell line, we report all off-target variants with a variant allele frequency (VAF) greater
781 than 0.7 and read depth greater than 5.

782

783 **References**

784 1. Vartanyan, S. L., Arslanov, K. A., Karhu, J. A., Possnert, G. & Sulerzhitsky, L. D. Collection
785 of radiocarbon dates on the mammoths (*Mammuthus Primigenius*) and other genera of
786 Wrangel Island, northeast Siberia, Russia. *Quat. Res.* **70**, 51–59 (2008).
787 2. Dehasque, M. *et al.* Temporal dynamics of woolly mammoth genome erosion prior to
788 extinction. *Cell* **187**, 3531-3540.e13 (2024).
789 3. Díez-Del-Molino, D. *et al.* Genomics of adaptive evolution in the woolly mammoth. *Curr.*
790 *Biol. CB* **33**, 1753-1764.e4 (2023).
791 4. Shapiro, B. Pathways to de-extinction: how close can we get to resurrection of an extinct
792 species? *Funct. Ecol.* **31**, 996–1002 (2017).
793 5. Wang, H. *et al.* One-step generation of mice carrying mutations in multiple genes by
794 CRISPR/Cas-mediated genome engineering. *Cell* **153**, 910–918 (2013).
795 6. Williams, A., Henao-Mejia, J. & Flavell, R. A. Editing the Mouse Genome Using the
796 CRISPR-Cas9 System. *Cold Spring Harb. Protoc.* **2016**, pdb.top087536 (2016).
797 7. Cong, L. *et al.* Multiplex genome engineering using CRISPR/Cas systems. *Science* **339**,
798 819–823 (2013).
799 8. Komor, A. C., Kim, Y. B., Packer, M. S., Zuris, J. A. & Liu, D. R. Programmable editing of a
800 target base in genomic DNA without double-stranded DNA cleavage. *Nature* **533**, 420–424
801 (2016).
802 9. Gaudelli, N. M. *et al.* Programmable base editing of A•T to G•C in genomic DNA without
803 DNA cleavage. *Nature* **551**, 464–471 (2017).
804 10. Anzalone, A. V. *et al.* Search-and-replace genome editing without double-strand breaks or
805 donor DNA. *Nature* **576**, 149–157 (2019).
806 11. Bradley, A., Evans, M., Kaufman, M. H. & Robertson, E. Formation of germ-line chimaeras
807 from embryo-derived teratocarcinoma cell lines. *Nature* **309**, 255–256 (1984).

808 12. Zuo, E. *et al.* One-step generation of complete gene knockout mice and monkeys by
809 CRISPR/Cas9-mediated gene editing with multiple sgRNAs. *Cell Res.* **27**, 933–945 (2017).
810 13. Teixeira, M. *et al.* Electroporation of mice zygotes with dual guide RNA/Cas9 complexes for
811 simple and efficient cloning-free genome editing. *Sci. Rep.* **8**, 474 (2018).
812 14. Mehravar, M., Shirazi, A., Nazari, M. & Banan, M. Mosaicism in CRISPR/Cas9-mediated
813 genome editing. *Dev. Biol.* **445**, 156–162 (2019).
814 15. Sakurai, T. *et al.* Production of genetically engineered mice with higher efficiency, lower
815 mosaicism, and multiplexing capability using maternally expressed Cas9. *Sci. Rep.* **10**, 1091
816 (2020).
817 16. Poueymirou, W. T. *et al.* F0 generation mice fully derived from gene-targeted embryonic
818 stem cells allowing immediate phenotypic analyses. *Nat. Biotechnol.* **25**, 91–99 (2007).
819 17. Sumiyama, K. *et al.* Easy and efficient production of completely embryonic-stem-cell-derived
820 mice using a micro-aggregation device. *PloS One* **13**, e0203056 (2018).
821 18. Makkar, J. *et al.* Deep Hair Phenomics: Implications in Endocrinology, Development, and
822 Aging. *J. Invest. Dermatol.* **145**, 800-811.e8 (2025).
823 19. Castro, A. R., Portinha, C. & Logarinho, E. The Emergent Power of Human Cellular vs
824 Mouse Models in Translational Hair Research. *Stem Cells Transl. Med.* **11**, 1021–1028
825 (2022).
826 20. Tridico, S. R., Rigby, P., Kirkbride, K. P., Haile, J. & Bunce, M. Megafaunal split ends:
827 microscopical characterisation of hair structure and function in extinct woolly mammoth and
828 woolly rhino. *Quat. Sci. Rev.* **83**, 68–75 (2014).
829 21. Hébert, J. M., Rosenquist, T., Götz, J. & Martin, G. R. FGF5 as a regulator of the hair
830 growth cycle: evidence from targeted and spontaneous mutations. *Cell* **78**, 1017–1025
831 (1994).
832 22. Brennan, B. M. *et al.* The mouse wellhaarig (we) mutations result from defects in epidermal-
833 type transglutaminase 3 (Tgm3). *Mol. Genet. Metab.* **116**, 187–191 (2015).

834 23. Radden, L. A. *et al.* The wooly mutation (wly) on mouse chromosome 11 is associated with
835 a genetic defect in Fam83g. *BMC Res. Notes* **6**, 189 (2013).
836 24. Guo, N., Hawkins, C. & Nathans, J. Frizzled6 controls hair patterning in mice. *Proc. Natl.*
837 *Acad. Sci.* **101**, 9277–9281 (2004).
838 25. Du, X., Li, X., Smart, N. G., La Vine, D. & Beutler, B. Mutagenetix 'Plush'. *MUTAGENETIX*
839 https://mutagenetix.utsouthwestern.edu/phenotypic/phenotypic_rec.cfm?pk=96 (2011).
840 26. Du, X., Li, X., Smart, N. G., La Vine, D. & Beutler, B. Mutagenetix 'Rough-fur'.
841 *MUTAGENETIX*
842 https://mutagenetix.utsouthwestern.edu/phenotypic/phenotypic_rec.cfm?pk=144 (2010).
843 27. Mann, G. B. *et al.* Mice with a null mutation of the TGF alpha gene have abnormal skin
844 architecture, wavy hair, and curly whiskers and often develop corneal inflammation. *Cell* **73**,
845 249–261 (1993).
846 28. Robbins, L. Pigmentation phenotypes of variant extension locus alleles result from point
847 mutations that alter MSH receptor function. *Cell* **72**, 827–834 (1993).
848 29. Fontaine, D. A. & Davis, D. B. Attention to Background Strain Is Essential for Metabolic
849 Research: C57BL/6 and the International Knockout Mouse Consortium. *Diabetes* **65**, 25–33
850 (2016).
851 30. 000686 - SJL Strain Details. https://www.jax.org/strain/000686.
852 31. Brilliant, M. H. The mouse p (pink-eyed dilution) and human P genes, oculocutaneous
853 albinism type 2 (OCA2), and melanosomal pH. *Pigment Cell Res.* **14**, 86–93 (2001).
854 32. Shoji, H. *et al.* A nonsense nucleotide substitution in the oculocutaneous albinism II gene
855 underlies the original pink-eyed dilution allele (Oca2p) in mice. *Exp. Anim.* **64**, 171–179
856 (2015).
857 33. Fur, N. L., Kelsall, S. R. & Mintz, B. Base Substitution at Different Alternative Splice Donor
858 Sites of the Tyrosinase Gene in Murine Albinism. *Genomics* **37**, 245–248 (1996).

859 34. Silvers, W. K. The Agouti and Extension Series of Alleles, Umbrous, and Sable. in *The Coat*
860 *Colors of Mice: A Model for Mammalian Gene Action and Interaction* (ed. Silvers, W. K.) 6–
861 44 (Springer, New York, NY, 1979). doi:10.1007/978-1-4612-6164-3_2.
862 35. Ollmann, M. M., Lamoreux, M. L., Wilson, B. D. & Barsh, G. S. Interaction of Agouti protein
863 with the melanocortin 1 receptor in vitro and in vivo. *Genes Dev.* **12**, 316–330 (1998).
864 36. Benned-Jensen, T., Mokrosinski, J. & Rosenkilde, M. M. The E92K Melanocortin 1 Receptor
865 Mutant Induces cAMP Production and Arrestin Recruitment but Not ERK Activity Indicating
866 Biased Constitutive Signaling. *PLoS ONE* **6**, e24644 (2011).
867 37. Moreland, K. *et al.* Deep-time genomics reveals the evolution of distinct genetic variants in
868 the woolly mammoth (Manuscript in preparation). (2025).
869 38. Agellon, L. B. *et al.* Loss of intestinal fatty acid binding protein increases the susceptibility of
870 male mice to high fat diet-induced fatty liver. *Biochim. Biophys. Acta BBA - Mol. Cell Biol.*
871 *Lipids* **1771**, 1283–1288 (2007).
872 39. Chen, Y. & Agellon, L. B. Distinct Alteration of Gene Expression Programs in the Small
873 Intestine of Male and Female Mice in Response to Ablation of Intestinal Fabp Genes.
874 *Genes* **11**, 943 (2020).
875 40. Jeong, Y. K., Song, B. & Bae, S. Current Status and Challenges of DNA Base Editing Tools.
876 *Mol. Ther. J. Am. Soc. Gene Ther.* **28**, 1938–1952 (2020).
877 41. Kuscu, C. *et al.* CRISPR-STOP: gene silencing through base-editing-induced nonsense
878 mutations. *Nat. Methods* **14**, 710–712 (2017).
879 42. Chang, H., Cahill, H., Smallwood, P. M., Wang, Y. & Nathans, J. Identification of
880 Astrotactin2 as a Genetic Modifier That Regulates the Global Orientation of Mammalian Hair
881 Follicles. *PLoS Genet.* **11**, e1005532 (2015).
882 43. Kluesner, M. G. *et al.* CRISPR-Cas9 cytidine and adenosine base editing of splice-sites
883 mediates highly-efficient disruption of proteins in primary and immortalized cells. *Nat.*
884 *Commun.* **12**, 2437 (2021).

885 44. Walton, R. T., Christie, K. A., Whittaker, M. N. & Kleinstiver, B. P. Unconstrained genome
886 targeting with near-PAMless engineered CRISPR-Cas9 variants. *Science* **368**, 290–296
887 (2020).
888 45. Hibshman, G. N. *et al.* Unraveling the mechanisms of PAMless DNA interrogation by SpRY-
889 Cas9. *Nat. Commun.* **15**, 3663 (2024).
890 46. Huang, Y. *et al.* A molecular mechanism for the generation of ligand-dependent differential
891 outputs by the epidermal growth factor receptor. *eLife* **10**, e73218 (2021).
892 47. MGI Krt27. https://www.informatics.jax.org/allele/MGI:3522000 (2005).
893 48. Tálas, A. *et al.* BEAR reveals that increased fidelity variants can successfully reduce the
894 mismatch tolerance of adenine but not cytosine base editors. *Nat. Commun.* **12**, 6353
895 (2021).
896 49. Gaztelumendi, N. & Nogués, C. Chromosome Instability in mouse Embryonic Stem Cells.
897 *Sci. Rep.* **4**, 5324 (2014).
898 50. Ukai, H., Kiyonari, H. & Ueda, H. R. Production of knock-in mice in a single generation from
899 embryonic stem cells. *Nat. Protoc.* **12**, 2513–2530 (2017).
900 51. Funano, S., Tone, D., Ukai, H., Ueda, H. R. & Tanaka, Y. Rapid and easy-to-use ES cell
901 manipulation device with a small groove near culturing wells. *BMC Res. Notes* **13**, 453
902 (2020).
903 52. Crew, F. A. E. & Auerbach, Ch. Rex: A dominant autosomal monogenic coat texture
904 character in the mouse. *J. Genet.* **38**, 341–344 (1939).
905 53. McFarlane, L., Truong, V., Palmer, J. S. & Wilhelm, D. Novel PCR assay for determining the
906 genetic sex of mice. *Sex. Dev. Genet. Mol. Biol. Evol. Endocrinol. Embryol. Pathol. Sex*
907 *Determ. Differ.* **7**, 207–211 (2013).
908 54. Hwang, S. M. *et al.* The application of an in situ karyotyping technique for mesenchymal
909 stromal cells: a validation and comparison study with classical G-banding. *Exp. Mol. Med.*
910 **45**, e68 (2013).

911 55. Borgonovo, T., Vaz, I. M., Senegaglia, A. C., Rebelatto, C. L. K. & Brofman, P. R. S.
912 Genetic evaluation of mesenchymal stem cells by G-banded karyotyping in a Cell
913 Technology Center. *Rev. Bras. Hematol. E Hemoter.* **36**, 202–207 (2014).
914 56. Wu, J. *et al.* An alternative pluripotent state confers interspecies chimaeric competency.
915 *Nature* **521**, 316–321 (2015).
916 57. Ying, Q.-L. *et al.* The ground state of embryonic stem cell self-renewal. *Nature* **453**, 519–
917 523 (2008).
918 58. Doench, J. G. *et al.* Optimized sgRNA design to maximize activity and minimize off-target
919 effects of CRISPR-Cas9. *Nat. Biotechnol.* **34**, 184–191 (2016).
920 59. Neugebauer, M. E. *et al.* Evolution of an adenine base editor into a small, efficient cytosine
921 base editor with low off-target activity. *Nat. Biotechnol.* **41**, 673–685 (2023).
922 60. Chen, S., Zhou, Y., Chen, Y. & Gu, J. fastp: an ultra-fast all-in-one FASTQ preprocessor.
923 *Bioinformatics* **34**, i884–i890 (2018).
924 61. Boratyn, G. M., Thierry-Mieg, J., Thierry-Mieg, D., Busby, B. & Madden, T. L. Magic-BLAST,
925 an accurate RNA-seq aligner for long and short reads. *BMC Bioinformatics* **20**, 405 (2019).
926 62. Genome assembly GRCm39.
927 https://www.ncbi.nlm.nih.gov/datasets/genome/GCF_000001635.27/ (2020).
928 63. Li, H. Aligning sequence reads, clone sequences and assembly contigs with BWA-MEM.
929 Preprint at https://doi.org/10.48550/ARXIV.1303.3997 (2013).
930 64. Freed, D., Aldana, R., Weber, J. A. & Edwards, J. S. The Sentieon Genomics Tools - A fast
931 and accurate solution to variant calling from next-generation sequence data. Preprint at
932 https://doi.org/10.1101/115717 (2017).
933 65. Hoberecht, L., Perampalam, P., Lun, A. & Fortin, J.-P. A comprehensive Bioconductor
934 ecosystem for the design of CRISPR guide RNAs across nucleases and technologies. *Nat.*
935 *Commun.* **13**, 6568 (2022).
936

Supplemental Figures

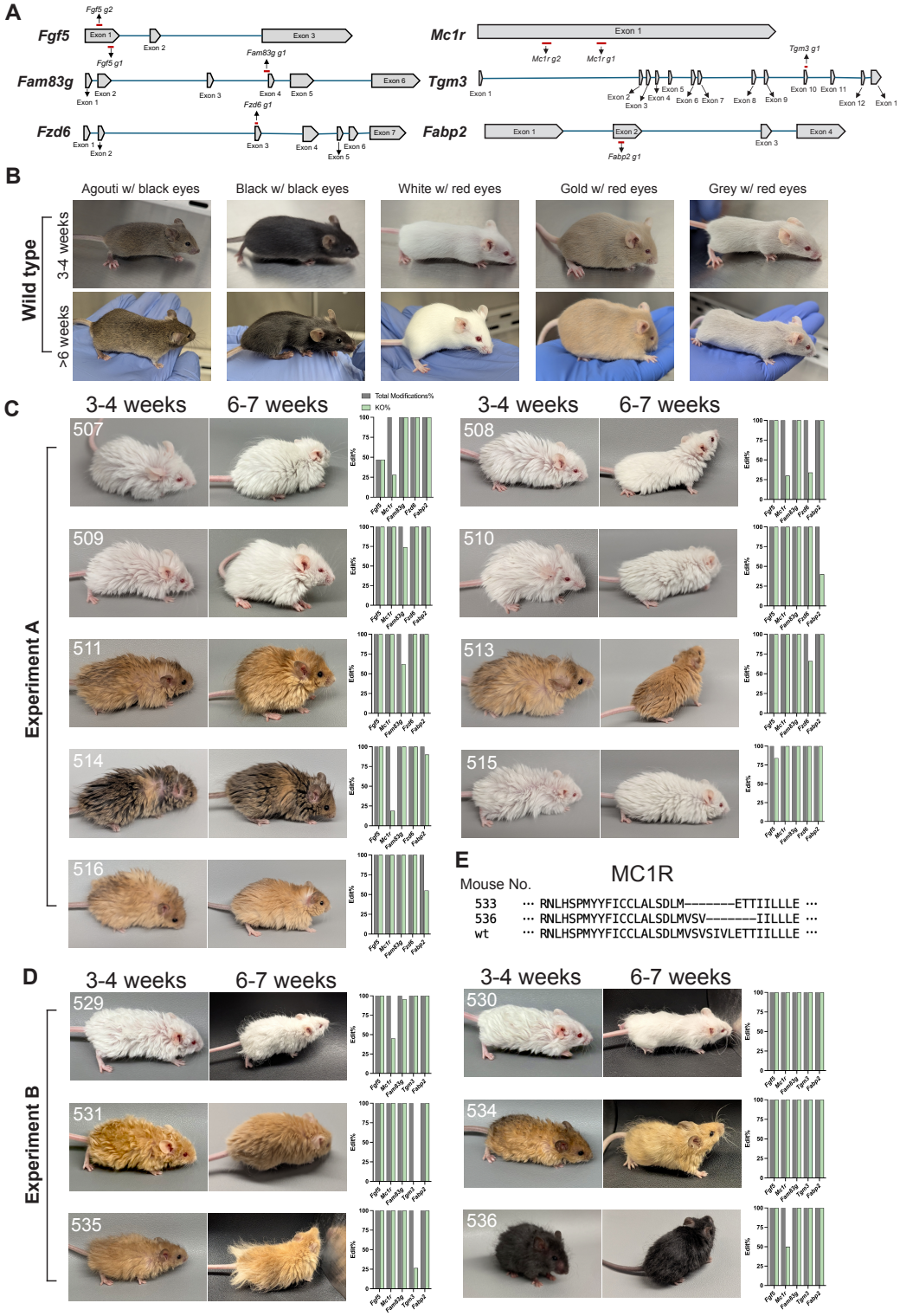

Figure S1. Multiplex Editing of Zygotes with CRISPR/Cas9, related to Figure 2. (A) Target genes and the location of their sgRNAs chosen for Cas9 KO animal production. We selected production sgRNA

941 according to editing efficiency, off-target prediction, and the location of the edit. The ideal edit location
942 should either mimic the previous literature or be in an early exon to facilitate KO. **(B)** Wild-type B6SJL F2
943 mice (B6 × SJL)F1 × (B6 × SJL)F1 have a variety of coat+eye color combinations: agouti with black eyes
944 (the most common), black with black eyes, white with red eyes, gold with red eyes (rare), and diluted grey
945 with red eyes (rare). Two age points are shown here. The agouti mouse pictures are the same as used in
946 Fig. 2 and Fig. 3. **(C, D)** The editing profiles and photos of mice not shown in Fig. 2 from Cas9 KO
947 Experiment A and B. **(E**) Alignment of the two different types of 7-amino-acid deletions in MC1R (from
948 mouse #533 and #536) with the wild-type MC1R protein sequence.

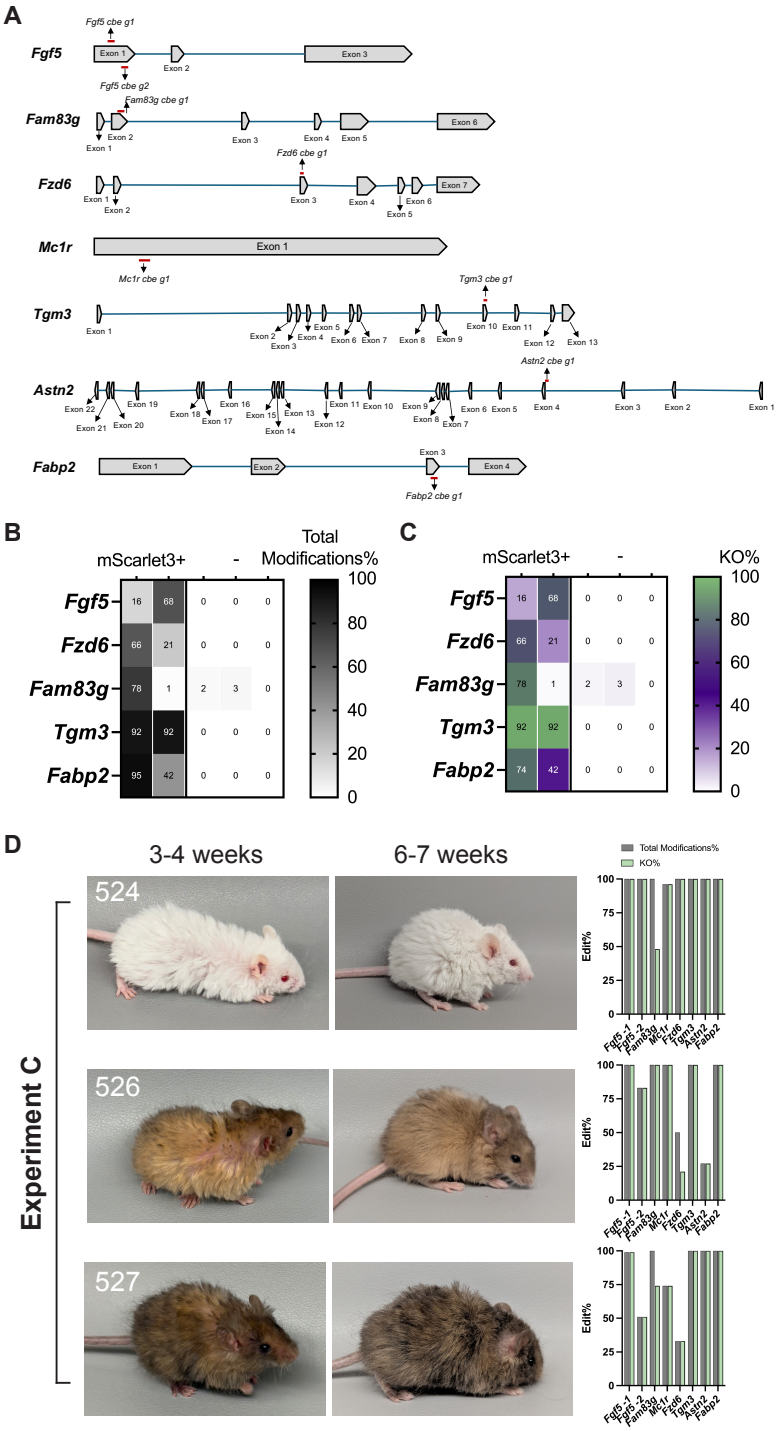

Figure S2. Multiplex Editing of Zygotes with CBE, related to Figure 3. (A) Target genes and the location of their sgRNAs chosen for CBE KO animal production. We selected animal production sgRNA according to editing efficiency, off-target prediction, and the location of the C-to-T mutation. The ideal edit location should either mimic the previous literature or be in an early exon to facilitate KO. **(B, C)** Single embryo total modification% and KO% comparison between mScarlet3 + and mScarlet3 - embryos demonstrated in Figure 3C. The individualized data represent the multiplexability and editing mosaicism in one animal by each condition. Each column is data from 1 embryo. Editing was determined by Sanger sequencing. **(D)** The editing profiles and photos of mice not shown in Figure 3 (Experiment C).

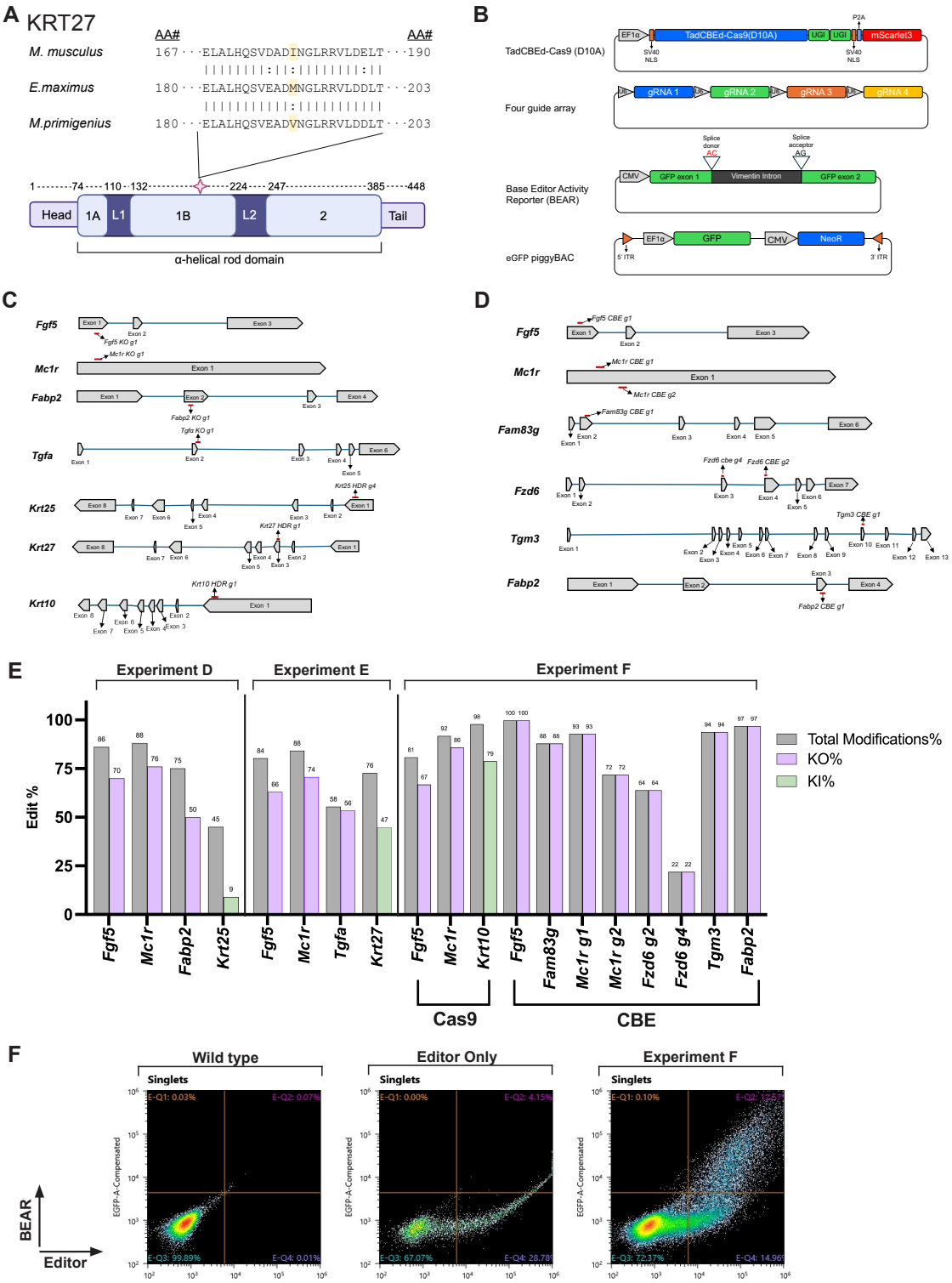

Figure S3. Multi-modality multiplex editing in mESC, related to Figure 4. (A) KRT27 protein alignment of *Mus musculus, Elephas maximus,* and *Mammuthus primigenius* centered around amino acid (AA) 191 (highlighted in yellow), a fixed coding mutation between *E. maximus* (methionine) and *M. primigenius* (valine). In Experiment E, the *M. musculus* isoleucine was edited to *M. primigenius* valine via HDR. This

963 mutation occurs in the 1B α-helical rod domain of the secondary structure of the KRT27 protein (star). **(B)**
964 Maps of plasmids used in Experiment D, E, and F. **(C)** Target genes and the location of the sgRNAs
965 selected for Cas9 KO and Cas9 HDR mESC generation. **(D)** Target genes and the location of the sgRNAs
966 selected for CBE KO mESC generation. **(E)** The KO% and KI% from Experiment D, E, and F bulk mESC
967 populations prior to single-cell sorting. **(F)** Gating strategy for single cell sorting Experiment F mESCs. First,
968 we applied a size gate to select mESCs and remove iMEF carryover, followed by another size gate to
969 exclude doublets. In the singlet gate, a quadrant gate was created to divide the diagram into four quadrants
970 named Q1, Q2, Q3, Q4. Experiment F mESCs falling in Q2 (CBE editor (+) and BEAR (+)) were selected
971 for single cell isolation.

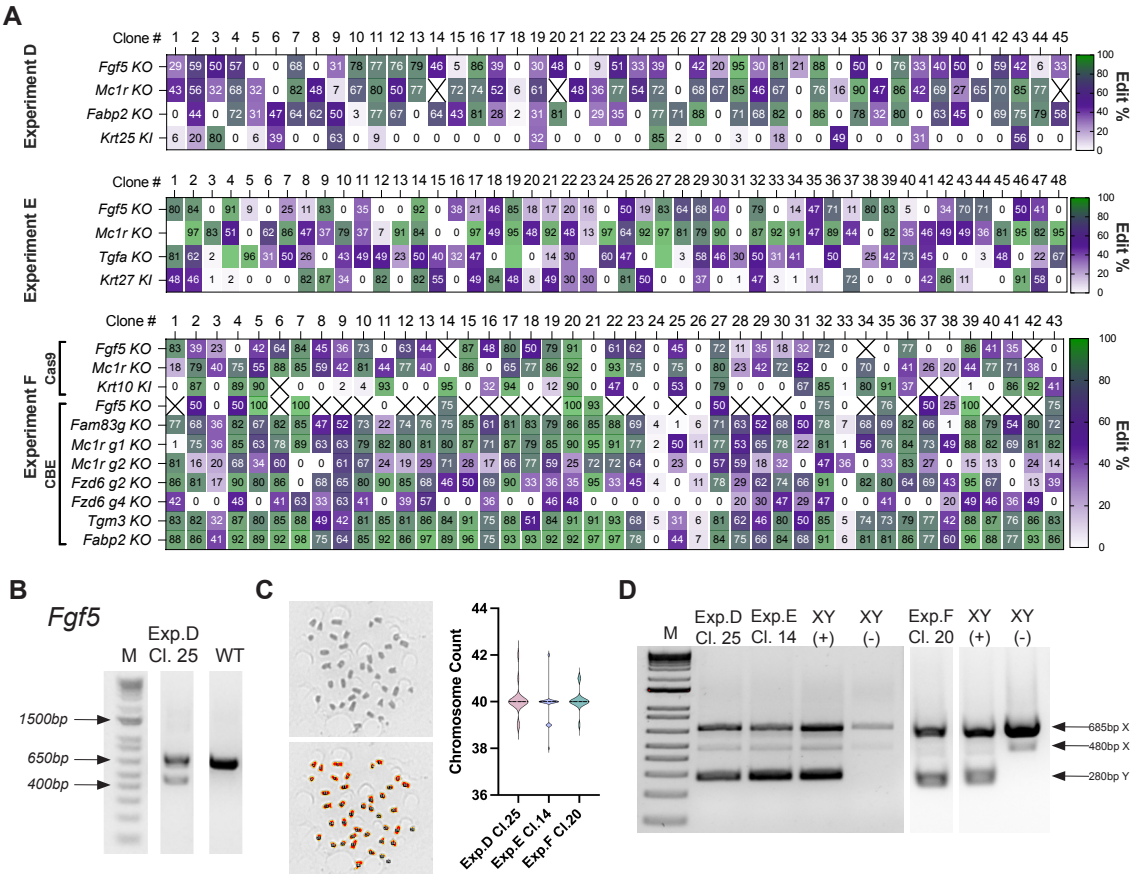

Figure S4. Clonal isolation of highly edited mESCs with normal chromosomal profiles, related to Figure 4. (A) Preliminary KO and KI editing profiles for 45 clones generated in Experiment D, 48 clones generated in Experiment E, and 43 clones generated in Experiment F. We collected clones from an iMEF feeder layer and genotyped rapidly by Sanger sequencing. "X" marked the genotyping dropouts which was uninterpretable from Sanger results. The remaining data was sufficient to determine high value clones for further validations. **(B)** PCR analysis of *Fgf5* from Experiment D, clone 25, which shows a large deletion that was not initially identified by ICE analysis. The DNA ladder marker is labeled as "M". **(C)** Representative mESC metaphase spread used for chromosome counting. Images were acquired using an EVOS M7000 with 20X objective. Upper left is the original photo (greyscale); lower left is the same photo where chromosomes were recognized (highlighted by colors) and counted by ImageJ. We counted chromosomes from n = 20 (Experiment D), n = 29 (Experiment E), and n = 17 (Experiment F) edited mESCs. Experiment D, clone 25, was 80% normal with an average count of 40.1 chromosomes and median count of 40 chromosomes. Experiment E, clone 14, was 70% normal with an average count of 39.90 chromosomes and median count of 40 chromosomes. Experiment F, clone 20, was 83% normal with an average count of 40.1 chromosomes and median count of 40 chromosomes. **(D)** XY PCR of Experiments D/E/F edited mESCs used for animal generation. The positive control (+) and negative control (-) are mESC lines characterized previously for internal use.

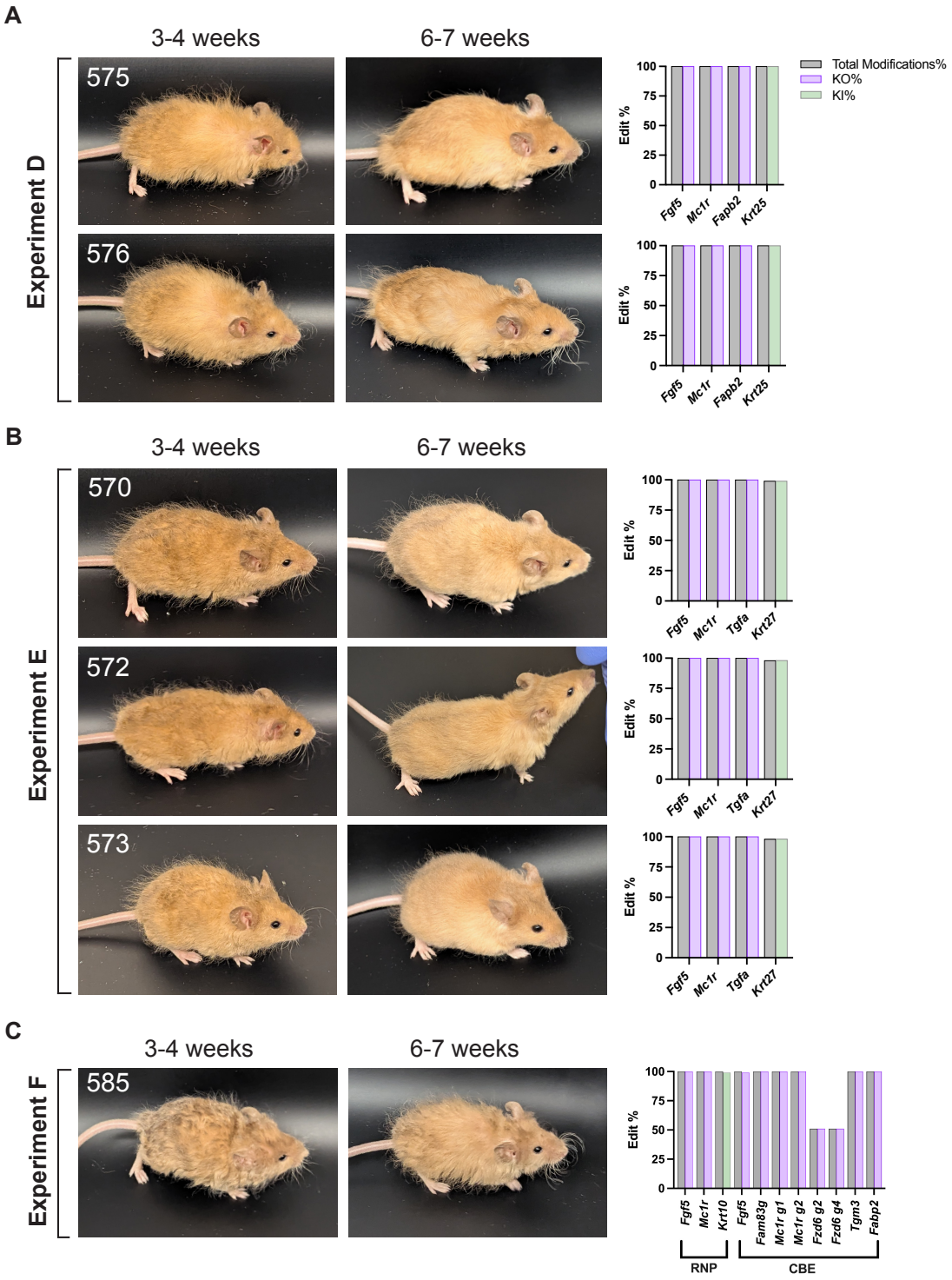

Figure S5. Near full mESC contribution mice produced by high yield chimera, related to Figure 5. (A-C) Editing profiles and photos of mice generated from Experiment D, E, and F mESCs not shown in Figure 5.

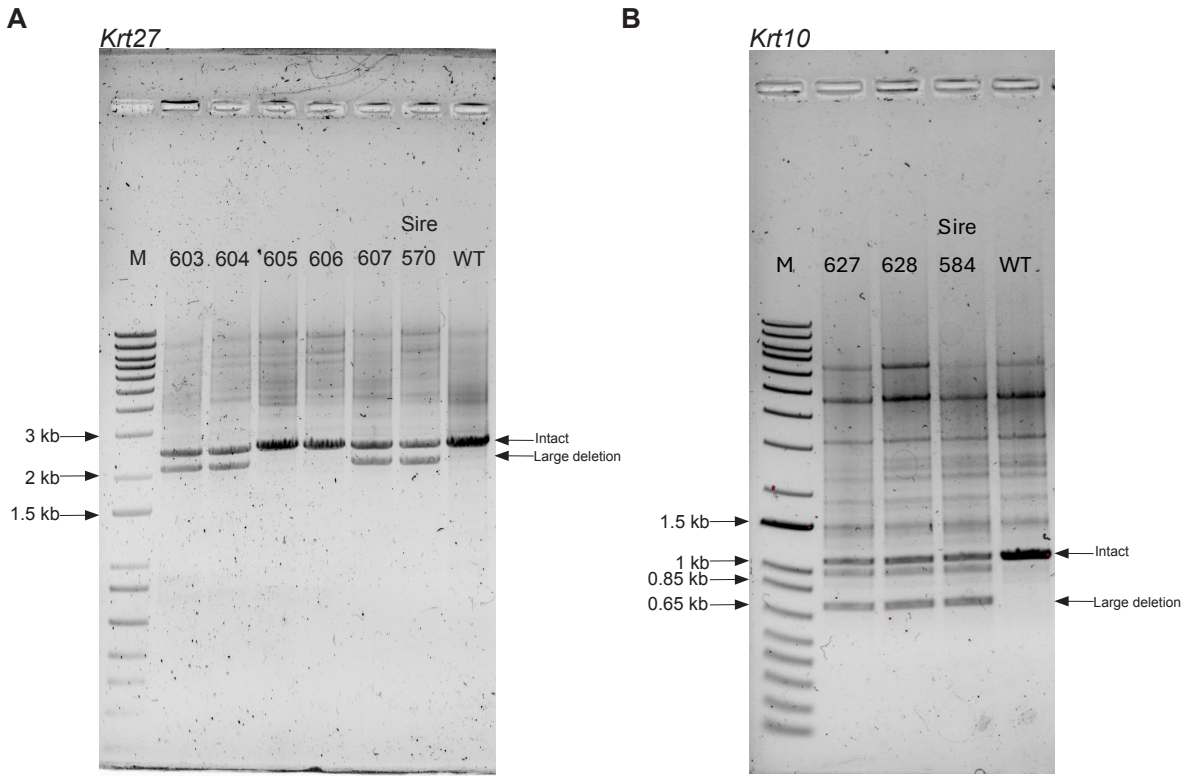

Figure S6. Previously undetected large deletion from Cas9 HDR editing and hemizygosity inheritance by the F1 progenies, related to Figure 6. PCR analysis of *Krt27* and *Krt10* genotypes on the F0 sire and WT cross-breeding progeny from Experiment E and F. The sires (#570 for *Krt27*; #584 for *Krt10*) show a large deletion on one allele that was not discovered by NGS before the breeding scheme. The large deletion also showed up in some progenies (#603, #604, and #607 for *Krt27*; #627 and #628 for *Krt10*), correlating with their lack of *Krt27 KI* or *Krt10 KI* allele in Figure 6D. On the contrary, progeny #605 and #606 exhibited one normal size band, correlating with the heterozygous *Krt27 KI* genotype. The DNA ladder marker is labeled as “M”.

1005 **Supplemental Tables**
1006
1007 **Table S1. Trait engineering target genes in this study, related to Figure 1.**

Gene	Expected Phenotype	Edit type	Modality used	Workflow		Experiment
Astn2	Ridge hair	Exon-skip	CBE	Zygote editing		C
Fam83g	Woolly hair	KO	Cas9; CBE	Zygote editing	High efficiency chimera	A B C F
Fzd6	Disoriented hair	KO	Cas9; CBE	Zygote editing	High efficiency chimera	A C F
Tgm3	Curly hair	KO	Cas9; CBE	Zygote editing	High efficiency chimera	B C F
Fgf5	Long hair	KO	Cas9; CBE	Zygote editing	High efficiency chimera	A B C D E F
Mc1r	Gold hair	KO	Cas9; CBE	Zygote editing	High efficiency chimera	A B C D E F
Fabp2	Lipid metabolism; Mammoth-motivated	KO	Cas9; CBE	Zygote editing	High efficiency chimera	A B C D F
Tgfα	Wavy hair	KO	Cas9		High efficiency chimera	E
Krt25	Curly hair	KI	Cas9 HDR		High efficiency chimera	D
Krt27	Textured hair; Mammoth-motivated	KI	Cas9 HDR		High efficiency chimera	E
Krt10	Wavy hair	KI	Cas9 HDR		High efficiency chimera	F

1008
1009
1010

1011 **Table S2. Zygote and mESC editing animal production summary.**

Zygote editing Experiment	Strain background	Zygote Status	# Blastocyst/ # Injected zygotes (%)	# editor+/ # blastocyst (%)	# Recipients	# Pups born/ # transferred (%)	# Pups weaned / # Pups born (%)
A	(B6 × SJL)F1 × (B6 × SJL)F1	Fresh	63/134 (47)	NA	2	11/60 (18)	11/11 (100)
B		Fresh	42/75 (56)	NA	2	8/28 (29)	8/8 (100)
C		Fresh	78/111 (70)	51/78 (65)	3	5/47 (11)	5/5 (100)
	(B6 × C3H)F1 × (B6 × D2)F1	Thawed	46/65 (71)	16/46 (35)	1	3/9 (33)	3/3 (100)

1012

mESC Experiment	ES cell line	# Blastocysts developed / # Injected 8-cell embryos (%)	# Recipients	# Pups born / # transferred (%)	# Pups weaned / # Pups born (%)	# near 100% chimeras
D	Exp. D, clone 25	58 / 59 (98%)	3	6 / 58 (10%)	3 / 6 (50%)	3
E	Exp. E, clone 14	31 / 31 (100%)	2	5 / 31 (16%)	4 / 5 (80%)	4
F	Exp. F, clone 20	58 / 60 (97%)	3	2 / 58 (3%)	2 / 2 (100%)	2

1013

1014

1015 **Table S3. Off-target analysis summary from mESC clone unbiased WGS, related to Figure 4.**
1016

Clone	Impact	Variant Annotation	nVariants
Exp.D-clone 25	MODIFIER	intergenic_region	41
	MODIFIER	intron_variant	22
	MODIFIER	upstream_gene_variant	8
	MODIFIER	downstream_gene_variant	6
Exp.E-clone 14	MODERATE	missense_variant	1
	MODIFIER	intergenic_region	54
	MODIFIER	intron_variant	46
	MODIFIER	upstream_gene_variant	15
	MODIFIER	downstream_gene_variant	17
	MODIFIER	non_coding_transcript_exon_variant	2
Exp.F-clone 20	MODIFIER	intergenic_region	71
	MODIFIER	intron_variant	58
	MODIFIER	upstream_gene_variant	23
	MODIFIER	downstream_gene_variant	12

1017
1018 Missense variant detail

	Chr	Start	End	Gene	Ref	Alt	Annotation	VAF	Biotype
Exp.E-clone 14	chr11	107869130	107869130	*Prkca*	C	A	Missense variant	0.72	Protein coding

1019

1020 **Table S4. guide RNA and donor sequences used for mouse production experiments, related to**
1021 **Methods.**
1022 Guide RNA

Exp No.	Gene	Colossal Guide ID	Spacer	Names when two guides targeting the same genes was genotyped separately
A	*Fabp2*	MMG145	TCTGAAACTGACAATCACAC	
A	*Fam83g*	MMG83	TCTCCCAACACAGAATCTCA	
A	*Fgf5*	MMG189	TTTCCATCTGCAGATCTACC	
A	*Fgf5*	MMG67	AGGAACCCGGGAGACTCCAG	
A	*Fzd6*	MMG95	TTCATGTAGTTCTACCCTGT	
A	*Mc1r*	MMG113	AGAGCACGACGGGCTGTCGT	
B	*Fabp2*	MMG145	TCTGAAACTGACAATCACAC	
B	*Fam83g*	MMG83	TCTCCCAACACAGAATCTCA	
B	*Fgf5*	MMG189	TTTCCATCTGCAGATCTACC	
B	*Fgf5*	MMG67	AGGAACCCGGGAGACTCCAG	
B	*Mc1r*	MMG157	GGTAAGTGTCAGCATCGTGC	
B	*Tgm3*	MMG166	GCCTGGACCATCGTCTACAA	
C	*Astn2*	MMG177	TTCCCCCTGCAGAGAAGCAC	
C	*Fabp2*	MMG137	CTGTCCGAGAGGTTTCTGGT	
C	*Fam83g*	MMG100	TGCCTACCGAGGTGTGACCC	
C	*Fgf5*	MMG11	AAGGGCAACCCGCGCCTCCT	*Fgf5-1*
C	*Fgf5*	MMG12	TCTGCAGATCTACCCGGATG	*Fgf5-2*
C	*Fzd6*	MMG162	GCATCCGATGGCCTGAAGAA	
C	*Mc1r*	MMG160	TCCACTCAGGAGCCCCAGAA	
C	*Tgm3*	MMG116	GTGCACCAAAAGGCTTTGGA	
D	*Fabp2*	MMG145	TCTGAAACTGACAATCACAC	
D	*Fgf5*	MMG67	AGGAACCCGGGAGACTCCAG	
D	*Krt25*	MMG142	CGCTTGCACGTTGTCCAGGT	

D	*Mc1r*	MMG178	ATGGACACATACAGGCACCA	
E	*Fgf5*	MMG67	AGGAACCCGGGAGACTCCAG	
E	*Krt27*	MMG89	AGCGTCGATGCTGACATCAA	
E	*Mc1r*	MMG178	ATGGACACATACAGGCACCA	
E	*Tgfa*	MMG186	GATGGACTCACCACTCAGGG	
F	*Fabp2*	MMG137	CTGTCCGAGAGGTTTCTGGT	
F	*Fam83g*	MMG100	TGCCTACCGAGGTGTGACCC	
F	*Fgf5*	MMG67	AGGAACCCGGGAGACTCCAG	*Fgf5 Cas9*
F	*Fgf5*	MMG11	AAGGGCAACCCGCGCCTCCT	*Fgf5 CBE*
F	*Fzd6*	MMG106	TCAGATCAAGTCCCAAGAGA	*Fzd6 g2*
F	*Fzd6*	MMG103	AGAGCAAATTCATGTAGTTC	*Fzd6 g4*
F	*Krt10*	MMG71	AAGGAGTGGTACGAGAAGCA	
F	*Mc1r*	MMG178	ATGGACACATACAGGCACCA	
F	*Mc1r*	MMG160	TCCACTCAGGAGCCCCAGAA	*Mc1r g1*
F	*Mc1r*	MMG113	AGAGCACGACGGGCTGTCGT	*Mc1r g2*
F	*Tgm3*	MMG116	GTGCACCAAAAGGCTTTGGA	

HDR donors

Exp No.	**Gene**	**Colossal Donor ID**	**Sequence**
D	*Krt25*	DNR151	TGGCCTCCTGCAGCGCTTGCACGTTGTCCAGGTATGAG GCCTGGCGGTCATTAAGGTTCT
E	*Krt27*	DNR142	GGCACTCCACCAGAGCGTCGATGCTGACGTCAATGGCT TGCGGAGGGTCCTGGATGAGCT
F	*Krt10*	DNR131	GGAGGGTAAAATCAAGGAGTGGTACGTGAAGCATGGCA ACTCAAGCCAGCGAGAGCCCCGGGACTA

1026 **Table S5. guide RNA and donor sequence used in screening and testing experiments by figures,**
1027 **related to methods.**
1028 Guide RNA

Figure	Gene	Colossal Guide ID	Spacer	Name used in the related figures	Selected for mouse production?
Fig2B	*Fabp2*	MMG145	TCTGAAACTGACAATCACAC	*Fabp2 g1*	yes
Fig2B	*Fam83g*	MMG83	TCTCCCAACACAGAATCTCA	*Fam83g g1*	yes
Fig2B	*Fam83g*	MMG82	TCTCAGGGTACGCAGCAGCG	*Fam83g g2*	
Fig2B	*Fam83g*	MMG84	CATGCACCTGGGGCACCTCA	*Fam83g g3*	
Fig2B	*Fam83g*	MMG85	GAGCGGGCCCGCATGCACCT	*Fam83g g4*	
Fig2B	*Fgf5*	MMG189	TTTCCATCTGCAGATCTACC	*Fgf5 g1*	yes
Fig2B	*Fgf5*	MMG67	AGGAACCCGGGAGACTCCAG	*Fgf5 g2*	yes
Fig2B	*Fgf5*	MMG138	CAGGGGATTGTAGGAATACG	*Fgf5 g3*	
Fig2B	*Fgf5*	MMG139	AAATATTTGCTGTGTCTCAG	*Fgf5 g4*	
Fig2B	*Fzd6*	MMG95	TTCATGTAGTTCTACCCTGT	*Fzd6 g1*	yes
Fig2B	*Fzd6*	MMG96	TTGGTATAAAAGCTTGGCAA	*Fzd6 g2*	
Fig2B	*Mc1r*	MMG113	AGAGCACGACGGGCTGTCGT	*Mc1r g1*	yes
Fig2B	*Mc1r*	MMG157	GGTAAGTGTCAGCATCGTGC	*Mc1r g2*	yes
Fig2B	*Mc1r*	MMG155	TGGCTAGAAAGAAAGTGACG	*Mc1r g3*	
Fig2B	*Mc1r*	MMG156	CACAGATGAGCACGTCAATG	*Mc1r g4*	
Fig2B	*Mc1r*	MMG158	CCGCCAAGGCTTCTGCCTCA	*Mc1r g5*	
Fig2B	*Mc1r*	MMG159	CGCCAAGGCTTCTGCCTCAA	*Mc1r g6*	
Fig2B	*Mc1r*	MMG79	CCACCAACCAGTCAGAGCCT	*Mc1r g7*	
Fig2B	*Mc1r*	MMG80	CTGTATGTGTCCATCCCAGA	*Mc1r g8*	
Fig2B	*Tgm3*	MMG166	GCCTGGACCATCGTCTACAA	*Tgm3 g1*	yes
Fig2B	*Tgm3*	MMG165	GTACCCTTGTCCACGAAGTG	*Tgm3 g2*	
Fig2B	*Tgm3*	MMG164	GCTTGGTGCCACTCCGAGTG	*Tgm3 g3*	
Fig2B	*Tgm3*	MMG122	AAGGGTACCATTGTAGACGA	*Tgm3 g4*	
Fig2B	*Tgm3*	MMG121	TGACGATGAACATGACAGCC	*Tgm3 g5*	
Fig2B	*Tgm3*	MMG119	GATTTGAGATTTTCCCCACT	*Tgm3 g6*	
Fig3B	*Astn2*	MMG177	TTCCCCCTGCAGAGAAGCAC	*Astn2 cbe-g1*	yes
Fig3B	*Astn2*	MMG175	CCCCCTGCAGAGAAGCACCA	*Astn2 cbe-g2*	

Fig3B	*Astn2*	MMG176	TCCCCCTGCAGAGAAGCACC	*Astn2 cbe-g3*	
Fig3B	*Fabp2*	MMG137	CTGTCCGAGAGGTTTCTGGT	*Fabp2 cbe-g1*	yes
Fig3B	*Fam83g*	MMG100	TGCCTACCGAGGTGTGACCC	*Fam83g cbe-g1*	yes
Fig3B	*Fam83g*	MMG99	CCTACCGAGGTGTGACCCGG	*Fam83g cbe-g2*	
Fig3B	*Fam83g*	MMG102	CTTCACACGATCAGCCACCA	*Fam83g cbe-g3*	
Fig3B	*Fam83g*	MMG101	ACACGATCAGCCACCAAGTT	*Fam83g cbe-g4*	
Fig3B	*Fam83g*	MMG131	TCACACGATCAGCCACCAAG	*Fam83g cbe-g5*	
Fig3B	*Fgf5*	MMG11	AAGGGCAACCCGCGCCTCCT	*Fgf5 cbe-g1*	yes
Fig3B	*Fgf5*	MMG12	TCTGCAGATCTACCCGGATG	*Fgf5 cbe-g2*	yes
Fig3B	*Fgf5*	MMG140	GATTCCAAGAAAACAGCTAT	*Fgf5 cbe-g3*	
Fig3B	*Fgf5*	MMG136	GAATACGAGGAGTTTTCAGC	*Fgf5 cbe-g4*	
Fig3B	*Fzd6*	MMG162	GCATCCGATGGCCTGAAGAA	*Fzd6 cbe-g1*	yes
Fig3B	*Fzd6*	MMG153	CATCCGATGGCCTGAAGAAC	*Fzd6 cbe-g2*	
Fig3B	*Fzd6*	MMG152	TTGCCAAGCTTTTATACCAA	*Fzd6 cbe-g3*	
Fig3B	*Fzd6*	MMG154	CAGAGCAAATTCATGTAGTT	*Fzd6 cbe-g4*	
Fig3B	*Fzd6*	MMG151	ATCCGATGGCCTGAAGAACT	*Fzd6 cbe-g5*	
Fig3B	*Fzd6*	MMG132	TTTGCCAAGCTTTTATACCA	*Fzd6 cbe-g6*	
Fig3B	*Fzd6*	MMG103	AGAGCAAATTCATGTAGTTC	*Fzd6 cbe-g7*	
Fig3B	*Fzd6*	MMG105	CAGATCAAGTCCCAAGAGAC	*Fzd6 cbe-g8*	
Fig3B	*Fzd6*	MMG104	CTTTGCCAAGCTTTTATACC	*Fzd6 cbe-g9*	
Fig3B	*Fzd6*	MMG106	TCAGATCAAGTCCCAAGAGA	*Fzd6 cbe-g10*	
Fig3B	*Fzd6*	MMG135	TGACCAGGGGATCGCTGCTG	*Fzd6 cbe-g11*	
Fig3B	*Mc1r*	MMG160	TCCACTCAGGAGCCCCAGAA	*Mc1r cbe-g1*	yes
Fig3B	*Mc1r*	MMG158	CCGCCAAGGCTTCTGCCTCA	*Mc1r cbe-g2*	
Fig3B	*Mc1r*	MMG161	CCACTCAGGAGCCCCAGAAG	*Mc1r cbe-g3*	
Fig3B	*Mc1r*	MMG159	CGCCAAGGCTTCTGCCTCAA	*Mc1r cbe-g4*	
Fig3B	*Mc1r*	MMG113	AGAGCACGACGGGCTGTCGT	*Mc1r cbe-g5*	yes
Fig3B	*Mc1r*	MMG111	GTGCAGCAGCTGGACAACCT	*Mc1r cbe-g6*	
Fig3B	*Mc1r*	MMG112	GAGCACGACGGGCTGTCGTG	*Mc1r cbe-g7*	
Fig3B	*Tgm3*	MMG116	GTGCACCAAAAGGCTTTGGA	*Tgm3 cbe-g1*	yes
Fig3B	*Tgm3*	MMG115	GCACCAAAAGGCTTTGGACA	*Tgm3 cbe-g2*	

Fig3B	*Tgm3*	MMG163	CATCCGATTTGAGATTTTCC	*Tgm3 cbe-g3*	
Fig3B	*Tgm3*	MMG114	ATCCGATTTGAGATTTTCCC	*Tgm3 cbe-g4*	
Fig3B	*Tgm3*	MMG118	GACCTACCTTGCAACCACGG	*Tgm3 cbe-g5*	
Fig3B	*Tgm3*	MMG134	GGAAAGACAAGTGCACCAAA	*Tgm3 cbe-g6*	
Fig3B	*Tgm3*	MMG117	CCTACCTTGCAACCACGGGT	*Tgm3 cbe-g7*	
Fig3B	*Tgm3*	MMG133	GCATCCGATTTGAGATTTTC	*Tgm3 cbe-g8*	
Fig3D FigS2BC	*Fabp2*	MMG137	CTGTCCGAGAGGTTTCTGGT	*Fabp2*	yes
Fig3D FigS2BC	*Tgm3*	MMG116	GTGCACCAAAAGGCTTTGGA	*Tgm3*	yes
Fig3D FigS2BC	*Fgf5*	MMG12	TCTGCAGATCTACCCGGATG	*Fgf5*	yes
Fig3D FigS2BC	*Fzd6*	MMG132	TTTGCCAAGCTTTTATACCA	*Fzd6*	
Fig3D FigS2BC	*Fam83g*	MMG100	TGCCTACCGAGGTGTGACCC	*Fam83g*	yes
Fig4C	*Tgfa*	MMG186	GATGGACTCACCACTCAGGG	*Tgfa g1*	yes
Fig4C	*Tgfa*	MMG187	AACAGCACATCCCCCCTGAG	*Tgfa g2*	
Fig4C	*Tgfa*	MMG188	TATCCTGTTAGCTGTGTGCC	*Tgfa g3*	
Fig4C	*Tgfa*	MMG185	CAGAGCGAGCTGTCCGGTCG	*Tgfa g4*	
Fig4C	*Fgf5*	MMG67	AGGAACCCGGGAGACTCCAG	*Fgf5 g1*	yes
Fig4C	*Fgf5*	MMG139	AAATATTTGCTGTGTCTCAG	*Fgf5 g2*	
Fig4C	*Fgf5*	MMG138	CAGGGGATTGTAGGAATACG	*Fgf5 g3*	
Fig4C	*Mc1r*	MMG178	ATGGACACATACAGGCACCA	*Mc1r g1*	yes
Fig4C	*Mc1r*	MMG157	GGTAAGTGTCAGCATCGTGC	*Mc1r g2*	yes
Fig4C	*Mc1r*	MMG155	TGGCTAGAAAGAAAGTGACG	*Mc1r g3*	
Fig4C	*Mc1r*	MMG113	AGAGCACGACGGGCTGTCGT	*Mc1r g4*	yes
Fig4C	*Mc1r*	MMG80	CTGTATGTGTCCATCCCAGA	*Mc1r g5*	
Fig4C	*Mc1r*	MMG156	CACAGATGAGCACGTCAATG	*Mc1r g6*	
Fig4C	*Mc1r*	MMG79	CCACCAACCAGTCAGAGCCT	*Mc1r g7*	
Fig4C	*Krt25*	MMG142	CGCTTGCACGTTGTCCAGGT	*Krt25 g1*	yes
Fig4C	*Krt25*	MMG143	TTGCACGTTGTCCAGGTAGG	*Krt25 g2*	
Fig4C	*Krt27*	MMG89	AGCGTCGATGCTGACATCAA	*Krt27 g1*	yes

Fig4C	*Krt27*	MMG88	ATGCTGACATCAATGGCTTG	*Krt27 g2*	
Fig4C	*Krt10*	MMG71	AAGGAGTGGTACGAGAAGCA	*Krt10 g1*	
Fig4C	*Krt10*	MMG72	TGGAGGGTAAAATCAAGGAG	*Krt10 g2*	
Fig4D	*Fgf5*	MMG11	AAGGGCAACCCGCGCCTCCT	*Fgf5 cbe-g1*	yes
Fig4D	*Fgf5*	MMG140	GATTCCAAGAAAACAGCTAT	*Fgf5 cbe-g2*	
Fig4D	*Fgf5*	MMG136	GAATACGAGGAGTTTTCAGC	*Fgf5 cbe-g3*	
Fig4D	*Fam83g*	MMG100	TGCCTACCGAGGTGTGACCC	*Fam83g cbe-g1*	yes
Fig4D	*Fam83g*	MMG99	CCTACCGAGGTGTGACCCGG	*Fam83g cbe-g2*	
Fig4D	*Fam83g*	MMG102	CTTCACACGATCAGCCACCA	*Fam83g cbe-g3*	
Fig4D	*Fam83g*	MMG101	ACACGATCAGCCACCAAGTT	*Fam83g cbe-g4*	
Fig4D	*Fam83g*	MMG131	TCACACGATCAGCCACCAAG	*Fam83g cbe-g5*	
Fig4D	*Fzd6*	MMG135	TGACCAGGGGATCGCTGCTG	*Fzd6 cbe-g1*	
Fig4D	*Fzd6*	MMG106	TCAGATCAAGTCCCAAGAGA	*Fzd6 cbe-g2*	
Fig4D	*Fzd6*	MMG105	CAGATCAAGTCCCAAGAGAC	*Fzd6 cbe-g3*	
Fig4D	*Fzd6*	MMG103	AGAGCAAATTCATGTAGTTC	*Fzd6 cbe-g4*	
Fig4D	*Fzd6*	MMG132	TTTGCCAAGCTTTTATACCA	*Fzd6 cbe-g5*	
Fig4D	*Fzd6*	MMG104	CTTTGCCAAGCTTTTATACC	*Fzd6 cbe-g6*	
Fig4D	*Mc1r*	MMG160	TCCACTCAGGAGCCCCAGAA	*Mc1r cbe-g1*	yes
Fig4D	*Mc1r*	MMG113	AGAGCACGACGGGCTGTCGT	*Mc1r cbe-g2*	yes
Fig4D	*Mc1r*	MMG112	GAGCACGACGGGCTGTCGTG	*Mc1r cbe-g3*	
Fig4D	*Mc1r*	MMG111	GTGCAGCAGCTGGACAACCT	*Mc1r cbe-g4*	
Fig4D	*Tgm3*	MMG116	GTGCACCAAAAGGCTTTGGA	*Tgm3 cbe-g1*	yes
Fig4D	*Tgm3*	MMG115	GCACCAAAAGGCTTTGGACA	*Tgm3 cbe-g2*	
Fig4D	*Tgm3*	MMG134	GGAAAGACAAGTGCACCAAA	*Tgm3 cbe-g3*	
Fig4D	*Fabp2*	MMG137	CTGTCCGAGAGGTTTCTGGT	*Fabp2 cbe-g1*	yes

HDR donors

Figure	**Gene**	**Colossal Donor ID**	**Sequence**	**Name used in the related**	**Selected for mouse**

				figures	production?
Fig4C	*Krt25*	DNR151	TGGCCTCCTGCAGCGCTTGCAC GTTGTCCAGGTATGAGGCCTGG CGGTCATTAAGGTTCT	*d1*	yes
Fig4C	*Krt25*	DNR160	CCTTGATCTTCTGCTCCAGGTCA GCGTTGGCCTCCTGCAGCGCTT GCACGTTGTCCAGGTAGGAGGC CtGGCGGTCATTAAGGTTCTGCA TGGTCACCTTCTCATTGCCGGA GAGGAGCC	*d2*	
Fig4C	*Krt27*	DNR142	GGCACTCCACCAGAGCGTCGAT GCTGACgTCAATGGCTTGCGGA GGGTCCTGGATGAGCT	*d1*	yes
Fig4C	*Krt27*	DNR141	ACTGGCACTCCACCAGAGCGTC GATGCTGACgTCAATGGCTTGCG GAGGGTCCTGGATGAGCTGACC CTGTGCAGAACCG	*d2*	
Fig4C	*Krt10*	DNR131	GGAGGGTAAAATCAAGGAGTGG TACGtGAAGCATGGCAACTCAAG CCAGCGAGAGCCCCGGGACTA	*d1*	yes
Fig4C	*Krt10*	DNR132	TCTGGAAGAGTCAAACTACGAG CTGGAGGGTAAAATCAAGGAGT GGTACGtGAAGCATGGCAACTCA AGCCAGCGAGAGC	*d2*	

1031

1032 **Table S6. Genotyping primers for NGS and Sanger sequencing, related to Methods.**
1033
1034 Lower cases are NGS adaptor sequences.

Gene	Colossal Guide ID	Sanger Forward Primer	Sanger Reverse Primer	NGS Forward Primer	NGS Reverse Primer
Astn2	MMG175	AATACGCAGGGCAGTTCTGG	ATCAGGAGAAGCCCAGGGAT	tcgtcggcagcgtcagatgtgtataagagacagAATACGCAGGGCAGTTCTGG	gtctcgtgggctcggagatgtgtataagagacagATCAGGAGAAGCCCAGGGAT
Astn2	MMG176	AATACGCAGGGCAGTTCTGG	ATCAGGAGAAGCCCAGGGAT	tcgtcggcagcgtcagatgtgtataagagacagAATACGCAGGGCAGTTCTGG	gtctcgtgggctcggagatgtgtataagagacagATCAGGAGAAGCCCAGGGAT
Astn2	MMG177	AATACGCAGGGCAGTTCTGG	ATCAGGAGAAGCCCAGGGAT	tcgtcggcagcgtcagatgtgtataagagacagAATACGCAGGGCAGTTCTGG	gtctcgtgggctcggagatgtgtataagagacagATCAGGAGAAGCCCAGGGAT
Fabp2	MMG137	TTCCTATCATCCAGAGGGTCACT	ATCGCTTGGCCTCAACTCCT	tcgtcggcagcgtcagatgtgtataagagacagTCCAGAGGGTCACTGTGAGT	gtctcgtgggctcggagatgtgtataagagacagACTCAAAATCACCTTGTCTTTGGA
Fabp2	MMG145	AGCAAGGCAAAACAGAACTTGG	CCGTTCCGTCTGCTAGACTG	tcgtcggcagcgtcagatgtgtataagagacagAGCAAGGCAAAACAGAACTTGG	gtctcgtgggctcggagatgtgtataagagacagCCGTTCCGTCTGCTAGACTG
Fam83g	MMG100	GTATCGTGGAGGCCATCGAG	CTCCTGGGTCTGAGACGAGA	tcgtcggcagcgtcagatgtgtataagagacagGAACCCCAGGACAACGGAG	gtctcgtgggctcggagatgtgtataagagacagGTGAATGGGGGTCTCGCC
Fam83g	MMG101	TTCTCCACCTTGCACCTCAC	CCCAAGCTGCAGAGGAGAAT	tcgtcggcagcgtcagatgtgtataagagacagTTCTCCACCTTGCACCTCAC	gtctcgtgggctcggagatgtgtataagagacagCCCAAGCTGCAGAGGAGAAT
Fam83g	MMG102	TTCTCCACCTTGCACCTCAC	CCCAAGCTGCAGAGGAGAAT	tcgtcggcagcgtcagatgtgtataagagacagTTCTCCACCTTGCACCTCAC	gtctcgtgggctcggagatgtgtataagagacagCCCAAGCTGCAGAGGAGAAT

Fam83g	MMG131	TTCTCCACCTTGCACCTCAC	CCCAAGCTGCAGAGGAGAAT	tcgtcggcagcgtcagatgtgtataagagacagTTCTCCACCTTGCACCTCAC	gtctcgtgggctcggagatgtgtataagagacagCCCAAGCTGCAGAGGAGAAT
Fam83g	MMG82	TTCTCCACCTTGCACCTCAC	CCCAAGCTGCAGAGGAGAAT	tcgtcggcagcgtcagatgtgtataagagacagTTCTCCACCTTGCACCTCAC	gtctcgtgggctcggagatgtgtataagagacagCCCAAGCTGCAGAGGAGAAT
Fam83g	MMG83	TTCTCCACCTTGCACCTCAC	CCCAAGCTGCAGAGGAGAAT	tcgtcggcagcgtcagatgtgtataagagacagTTCTCCACCTTGCACCTCAC	gtctcgtgggctcggagatgtgtataagagacagCCCAAGCTGCAGAGGAGAAT
Fam83g	MMG84	CCCAGTCTTTTCCTGTTCCCA	TTGGTATAAGGCACTGTCTGC	tcgtcggcagcgtcagatgtgtataagagacagCCCAGTCTTTTCCTGTTCCCA	gtctcgtgggctcggagatgtgtataagagacagTTGGTATAAGGCACTGTCTGC
Fam83g	MMG85	CCCAGTCTTTTCCTGTTCCCA	TTGGTATAAGGCACTGTCTGC	tcgtcggcagcgtcagatgtgtataagagacagCCCAGTCTTTTCCTGTTCCCA	gtctcgtgggctcggagatgtgtataagagacagTTGGTATAAGGCACTGTCTGC
Fam83g	MMG99	GTATCGTGGAGGCCATCGAG	CTCCTGGGTCTGAGACGAGA	tcgtcggcagcgtcagatgtgtataagagacagGAACCCCAGGACAACGGAG	gtctcgtgggctcggagatgtgtataagagacagGTGAATGGGGGTCTCGCC
Fgf5	MMG11	GAGGCTATGTCCACCCTGTG	CACGAAACCCTACCGGACTC	tcgtcggcagcgtcagatgtgtataagagacagAAGATGCACTTAGGACCCCC	gtctcgtgggctcggagatgtgtataagagacagAAGGGCTCCACTGGAAACTG
Fgf5	MMG12	GAGGCTATGTCCACCCTGTG	CACGAAACCCTACCGGACTC	tcgtcggcagcgtcagatgtgtataagagacagGTAGCGCGACGTTTTCTTCG	gtctcgtgggctcggagatgtgtataagagacagGTCCCTCCCAGAACAGGTTT
Fgf5	MMG136	TCCGAGTGTACACGCATTGT	ACCGGTGGAGCACTTTTCAA	tcgtcggcagcgtcagatgtgtataagagacagGACATTGAATTCTTCACAGTTCTGTG	gtctcgtgggctcggagatgtgtataagagacagAACAATCTCTTCACTTTGTTACAGACG

Fgf5	MMG138	TCCGAGTGTACACG CATTGT	ACCGGTGGAGCA CTTTTCAA	tcgtcggcagcgtc agatgtgtataaga gacagGACATT GAATTCTTCA CAGTTCTGTG	gtctcgtgggctcgg agatgtgtataaga gacagAACAAT CTCTTCACTT TGTTACAGAC G
Fgf5	MMG139	TCCGAGTGTACACG CATTGT	ACCGGTGGAGCA CTTTTCAA	tcgtcggcagcgtc agatgtgtataaga gacagGACATT GAATTCTTCA CAGTTCTGTG	gtctcgtgggctcgg agatgtgtataaga gacagAACAAT CTCTTCACTT TGTTACAGAC G
Fgf5	MMG140	GGGAACAGAATAAG GGTATCCC	GTTTGACCCGTG GGCTGC	tcgtcggcagcgtc agatgtgtataaga gacagGGGAA CAGAATAAGG GTATCCC	gtctcgtgggctcgg agatgtgtataaga gacagGTTTGA CCCGTGGGC TGC
Fgf5	MMG189	GAGGCTATGTCCAC CCTGTG	CACGAAACCCTA CCGGACTC	tcgtcggcagcgtc agatgtgtataaga gacagTCTTCT GCCTCCTCAC CAGT	gtctcgtgggctcgg agatgtgtataaga gacagAGCAGA GTCCCAGAC GCTA
Fgf5	MMG67 300x NGS	GAGGCTATGTCCAC CCTGTG	CACGAAACCCTA CCGGACTC	tcgtcggcagcgtc agatgtgtataaga gacagAAGATG CACTTAGGAC CCCC	gtctcgtgggctcgg agatgtgtataaga gacagAAGGG CTCCACTGGA AACTG
Fgf5	MMG67, MMG189 500x NGS	GAGGCTATGTCCAC CCTGTG	CACGAAACCCTA CCGGACTC	tcgtcggcagcgtc agatgtgtataaga gacagAAGATG CACTTAGGAC CCCC	gtctcgtgggctcgg agatgtgtataaga gacagAGCAGA GTCCCAGAC GCTA
Fzd6	MMG103	GACTCATTTCGAAG GTAGGTGA	TTCTTCAGGCCAT CGGATGC	tcgtcggcagcgtc agatgtgtataaga gacagGACTCA TTTCGAAGGT AGGTGA	gtctcgtgggctcgg agatgtgtataaga gacagTTCTTC AGGCCATCG GATGC
Fzd6	MMG104	GACTCATTTCGAAG GTAGGTGA	TTCTTCAGGCCAT CGGATGC	tcgtcggcagcgtc agatgtgtataaga gacagGACTCA TTTCGAAGGT AGGTGA	gtctcgtgggctcgg agatgtgtataaga gacagTTCTTC AGGCCATCG GATGC
Fzd6	MMG105	GGAGTGAAGGGAAG GGGGAA	AGGAACGTGAAC AGAGTTGCA	tcgtcggcagcgtc agatgtgtataaga gacagTGTAAA CTTTACAGAT TGCCACAC	gtctcgtgggctcgg agatgtgtataaga gacagTACATA TTGGGGCAC GGAGG

Fzd6	MMG106	GGAGTGAAGGGAAG GGGGAA	AGGAACGTGAAC AGAGTTGCA	tcgtcggcagcgtc agatgtgtataaga gacagTGTAAA CTTTACAGAT TGCCACAC	gtctcgtgggctcgg agatgtgtataaga gacagTACATA TTGGGGCAC GGAGG
Fzd6	MMG132	GACTCATTTCGAAG GTAGGTGA	TTCTTCAGGCCAT CGGATGC	tcgtcggcagcgtc agatgtgtataaga gacagGACTCA TTTCGAAGGT AGGTGA	gtctcgtgggctcgg agatgtgtataaga gacagTTCTTC AGGCCATCG GATGC
Fzd6	MMG135	TGGCAAGATGGAAA GGTCCC	TTTCAATATAGGC ATGAAAATCCACT	tcgtcggcagcgtc agatgtgtataaga gacagTGGCAA GATGGAAAG GTCCC	gtctcgtgggctcgg agatgtgtataaga gacagTTTCAA TATAGGCATG AAAATCCACT
Fzd6	MMG151	TGAAATGTTCCTTTG CCAAGCT	ACGCGCTAACAA TACTAAAGTGC	tcgtcggcagcgtc agatgtgtataaga gacagTGAAAT GTTCCTTTGC CAAGCT	gtctcgtgggctcgg agatgtgtataaga gacagACGCG CTAACAATAC TAAAGTGC
Fzd6	MMG152	GACTCATTTCGAAG GTAGGTGA	TTCTTCAGGCCAT CGGATGC	tcgtcggcagcgtc agatgtgtataaga gacagGACTCA TTTCGAAGGT AGGTGA	gtctcgtgggctcgg agatgtgtataaga gacagTTCTTC AGGCCATCG GATGC
Fzd6	MMG153	TGAAATGTTCCTTTG CCAAGCT	ACGCGCTAACAA TACTAAAGTGC	tcgtcggcagcgtc agatgtgtataaga gacagTGAAAT GTTCCTTTGC CAAGCT	gtctcgtgggctcgg agatgtgtataaga gacagACGCG CTAACAATAC TAAAGTGC
Fzd6	MMG154	GACTCATTTCGAAG GTAGGTGA	TTCTTCAGGCCAT CGGATGC	tcgtcggcagcgtc agatgtgtataaga gacagGACTCA TTTCGAAGGT AGGTGA	gtctcgtgggctcgg agatgtgtataaga gacagTTCTTC AGGCCATCG GATGC
Fzd6	MMG162	TGAAATGTTCCTTTG CCAAGCT	ACGCGCTAACAA TACTAAAGTGC	tcgtcggcagcgtc agatgtgtataaga gacagTGAAAT GTTCCTTTGC CAAGCT	gtctcgtgggctcgg agatgtgtataaga gacagACGCG CTAACAATAC TAAAGTGC
Fzd6	MMG95	GACTCATTTCGAAG GTAGGTGA	TTCTTCAGGCCAT CGGATGC	tcgtcggcagcgtc agatgtgtataaga gacagGACTCA TTTCGAAGGT AGGTGA	gtctcgtgggctcgg agatgtgtataaga gacagTTCTTC AGGCCATCG GATGC

Fzd6	MMG96	GACTCATTTCGAAG GTAGGTGA	TTCTTCAGGCCAT CGGATGC	tcgtcggcagcgtc agatgtgtataaga gacagGACTCA TTTCGAAGGT AGGTGA	gtctcgtgggctcgg agatgtgtataaga gacagTTCTTC AGGCCATCG GATGC
Krt25	MMG142	TCCAATGCCCTTAAA TGCCC	TTCGCCTTTCCAG TGGATCC	tcgtcggcagcgtc agatgtgtataaga gacagTAGTCA TGATCGAGAC CGCG	gtctcgtgggctcgg agatgtgtataaga gacagTGTGCT GGCTTCACTG TGAA
Krt27	MMG89	GGAAGGTTGGGTGC CTACC	TGGGGTGACTCA AATCTGGC	tcgtcggcagcgtc agatgtgtataaga gacagGGAAG GTTGGGTGC CTACC	gtctcgtgggctcgg agatgtgtataaga gacagTGGGGT GACTCAAATC TGGC
Mc1r	MMG111	GAGACCCCCGACAA CAACAT	AGAAAGTGACGA GGCAGAGC	tcgtcggcagcgtc agatgtgtataaga gacagGCATCG TGCTGGAGA CTACT	gtctcgtgggctcgg agatgtgtataaga gacagAAGAGG GTGCTGGAG ACGAT
Mc1r	MMG112	GAGACCCCCGACAA CAACAT	AGAAAGTGACGA GGCAGAGC	tcgtcggcagcgtc agatgtgtataaga gacagGCATCG TGCTGGAGA CTACT	gtctcgtgggctcgg agatgtgtataaga gacagAAGAGG GTGCTGGAG ACGAT
Mc1r	MMG113	GAGACCCCCGACAA CAACAT	AGAAAGTGACGA GGCAGAGC	tcgtcggcagcgtc agatgtgtataaga gacagGCATCG TGCTGGAGA CTACT	gtctcgtgggctcgg agatgtgtataaga gacagAAGAGG GTGCTGGAG ACGAT
Mc1r	MMG155	TCCATCTTCTATGCG CTGCG	TTTTGTGGAGCTG GGCAATG	tcgtcggcagcgtc agatgtgtataaga gacagTCCATC TTCTATGCGC TGCG	gtctcgtgggctcgg agatgtgtataaga gacagTTTTGT GGAGCTGGG CAATG
Mc1r	MMG156	GAGACCCCCGACAA CAACAT	AGAAAGTGACGA GGCAGAGC	tcgtcggcagcgtc agatgtgtataaga gacagGCATCG TGCTGGAGA CTACT	gtctcgtgggctcgg agatgtgtataaga gacagAAGAGG GTGCTGGAG ACGAT
Mc1r	MMG157	GAGACCCCCGACAA CAACAT	AGAAAGTGACGA GGCAGAGC	tcgtcggcagcgtc agatgtgtataaga gacagGGAGC CCCAGAAGA GTCTTC	gtctcgtgggctcgg agatgtgtataaga gacagCCTCCA GCAGCAGGA TGATAG

Mc1r	MMG158	CTGCTCTGCCTCGTCACTTT	GGCAGAGGACGATGAGCAAG	tcgtcggcagcgtcagatgtgtataagagacagCTGCTCTGCCTCGTCACTTT	gtctcgtgggctcggagatgtgtataagagacagGGCAGAGGACGATGAGCAAG
Mc1r	MMG159	CTGCTCTGCCTCGTCACTTT	GGCAGAGGACGATGAGCAAG	tcgtcggcagcgtcagatgtgtataagagacagCTGCTCTGCCTCGTCACTTT	gtctcgtgggctcggagatgtgtataagagacagGGCAGAGGACGATGAGCAAG
Mc1r	MMG160	AAAATCGGAGCGTGCCTGTA	AAGGCTCTGACTGGTTGGTG	tcgtcggcagcgtcagatgtgtataagagacagAAAATCGGAGCGTGCCTGTA	gtctcgtgggctcggagatgtgtataagagacagAAGGCTCTGACTGGTTGGTG
Mc1r	MMG161	AAAATCGGAGCGTGCCTGTA	AAGGCTCTGACTGGTTGGTG	tcgtcggcagcgtcagatgtgtataagagacagAAAATCGGAGCGTGCCTGTA	gtctcgtgggctcggagatgtgtataagagacagAAGGCTCTGACTGGTTGGTG
Mc1r	MMG178	CTCCACAGACCGCTTCCTAC	ACCAGCACATTCTCCACCAG	tcgtcggcagcgtcagatgtgtataagagacagCTCCACAGACCGCTTCCTAC	gtctcgtgggctcggagatgtgtataagagacagACCAGCACATTCTCCACCAG
Mc1r	MMG79	GAGACCCCCGACAACAACAT	AGAAAGTGACGAGGCAGAGC	tcgtcggcagcgtcagatgtgtataagagacagGGAGCCCCAGAAGAGTCTTC	gtctcgtgggctcggagatgtgtataagagacagCCTCCAGCAGCAGGATGATAG
Mc1r	MMG80	GAGACCCCCGACAACAACAT	AGAAAGTGACGAGGCAGAGC	tcgtcggcagcgtcagatgtgtataagagacagGGAGCCCCAGAAGAGTCTTC	gtctcgtgggctcggagatgtgtataagagacagCCTCCAGCAGCAGGATGATAG
Tgfa	MMG186	CATCGAGCCCCTCAAAGGAG	TCCCTGGGAAGGAGCTTTCT	tcgtcggcagcgtcagatgtgtataagagacagCATCGAGCCCCTCAAAGGAG	gtctcgtgggctcggagatgtgtataagagacagTCCCTGGGAAGGAGCTTTCT
Tgm3	MMG114	AAGACTACCTGTCCCCTCCC	AGAAGTCCATGTCTGGCAGC	tcgtcggcagcgtcagatgtgtataagagacagCATGTAGCCTGAGCCCTCTG	gtctcgtgggctcggagatgtgtataagagacagGGGTCGGTCACTCAGAGACA

Tgm3	MMG115	TGGGAGCATTTTGGACAGGT	ATGCTGGGCTCCTTGTCTTC	tcgtcggcagcgtcagatgtgtataagagacagTGGGAGCATTTTGGACAGGT	gtctcgtgggctcggagatgtgtataagagacagATGCTGGGCTCCTTGTCTTC
Tgm3	MMG116	TGGGAGCATTTTGGACAGGT	ATGCTGGGCTCCTTGTCTTC	tcgtcggcagcgtcagatgtgtataagagacagTGGGAGCATTTTGGACAGGT	gtctcgtgggctcggagatgtgtataagagacagATGCTGGGCTCCTTGTCTTC
Tgm3	MMG117	CAACCCTCTGAGTCAGCCAG	CACAGCCAGGTAAGTGCAGA	tcgtcggcagcgtcagatgtgtataagagacagTCTGGCCATTGCTATTGCCA	gtctcgtgggctcggagatgtgtataagagacagCCACAGGCTTTCTCCAACCA
Tgm3	MMG118	CAACCCTCTGAGTCAGCCAG	CACAGCCAGGTAAGTGCAGA	tcgtcggcagcgtcagatgtgtataagagacagTCTGGCCATTGCTATTGCCA	gtctcgtgggctcggagatgtgtataagagacagCCACAGGCTTTCTCCAACCA
Tgm3	MMG119	AAGACTACCTGTCCCCTCCC	AGAAGTCCATGTCTGGCAGC	tcgtcggcagcgtcagatgtgtataagagacagCATGTAGCCTGAGCCCTCTG	gtctcgtgggctcggagatgtgtataagagacagGGGTCGGTCACTCAGAGACA
Tgm3	MMG121	ATGCACAGGTTCCAGTGAGG	AAGGCTTTACCCATGGAGGC	tcgtcggcagcgtcagatgtgtataagagacagGAAGGGGAAGACAAGGAGCC	gtctcgtgggctcggagatgtgtataagagacagGTGAGCAACTCTTTTGGGCC
Tgm3	MMG122	ATGCACAGGTTCCAGTGAGG	AAGGCTTTACCCATGGAGGC	tcgtcggcagcgtcagatgtgtataagagacagGAAGGGGAAGACAAGGAGCC	gtctcgtgggctcggagatgtgtataagagacagGTGAGCAACTCTTTTGGGCC
Tgm3	MMG133	AAGACTACCTGTCCCCTCCC	AGAAGTCCATGTCTGGCAGC	tcgtcggcagcgtcagatgtgtataagagacagCATGTAGCCTGAGCCCTCTG	gtctcgtgggctcggagatgtgtataagagacagGGGTCGGTCACTCAGAGACA
Tgm3	MMG134	TGGGAGCATTTTGGACAGGT	ATGCTGGGCTCCTTGTCTTC	tcgtcggcagcgtcagatgtgtataagagacagTGGGAGCATTTTGGACAGGT	gtctcgtgggctcggagatgtgtataagagacagATGCTGGGCTCCTTGTCTTC

Tgm3	MMG163	AAGACTACCTGTCCCCTCCC	AGAAGTCCATGTCTGGCAGC	tcgtcggcagcgtcagatgtgtataagagacagCATGTAGCCTGAGCCCTCTG	gtctcgtgggctcggagatgtgtataagagacagGGGTCGGTCACTCAGAGACA
Tgm3	MMG164	AAGACTACCTGTCCCCTCCC	AGAAGTCCATGTCTGGCAGC	tcgtcggcagcgtcagatgtgtataagagacagCATGTAGCCTGAGCCCTCTG	gtctcgtgggctcggagatgtgtataagagacagGGGTCGGTCACTCAGAGACA
Tgm3	MMG165	ATGCACAGGTTCCAGTGAGG	AAGGCTTTACCCATGGAGGC	tcgtcggcagcgtcagatgtgtataagagacagGAAGGGGAAGACAAGGAGCC	gtctcgtgggctcggagatgtgtataagagacagGTGAGCAACTCTTTTGGGCC
Tgm3	MMG166	ATGCACAGGTTCCAGTGAGG	AAGGCTTTACCCATGGAGGC	tcgtcggcagcgtcagatgtgtataagagacagGAAGGGGAAGACAAGGAGCC	gtctcgtgggctcggagatgtgtataagagacagGTGAGCAACTCTTTTGGGCC
Krt10	MMG71	GCATGCCTAGGAACGATGGA	GGTGACCATGCAGAACCTGA	tcgtcggcagcgtcagatgtgtataagagacagGCATGCCTAGGAACGATGGA	gtctcgtgggctcggagatgtgtataagagacagGGTGACCATGCAGAACCTGA

1035